

$R_{K^{(*)}}$ anomaly in type-III 2HDM**A. Arhrib^a R. Benbrik^{b,c,d} C. H. Chen^e J. K. Parry^d L. Rahili^f S. Semlali^g Q. S. Yan^{c,d}**^a*Abdelmalek Essaadi University, Faculty of Sciences and techniques, Tanger, Morocco*^b*MSISM Team, Faculté Polydisciplinaire de Safi, Sidi Bouzid, Morocco*^c*School of Physics Sciences, University of Chinese, Chinese Academy of Sciences, Beijing 100039, P.R. China*^d*Center for future high energy physics, Chinese Academy of Sciences, Beijing 100039, P.R. China*^e*Department of Physics, National Cheng-Kung University, Tainan 70101, Taiwan*^f*LMTI, Faculty of Sciences, Agadir University, B.P. 8106, Morocco.*^g*LPHEA, Faculty of Science Semlalia, Marrakech, 430079, Morocco.*^c*School of Physics Sciences, University of Chinese, Chinese Academy of Sciences, Beijing 100039, P.R. China**E-mail: aarhrib@gmail.com, r.benbrik@uca.ac.ma,
physchen@mail.ncku.edu.tw, jkparry@tsinghua.edu.cn,
rahililarbi@gmail.com, s.seemlali@gmail.com, yanqishu@ucas.ac.cn*

ABSTRACT: Recent experimental results provided by the CMS and LHCb, Belle and BaBar collaborations are showing a tension with the SM predictions in $R_{K^{(*)}}$, which might call for an explanation from new physics. In this work, we examine this tension in the type-III two-Higgs doublet models. We focus on the contributions of charged Higgs boson to the observable(s) $R_{K^{(*)}}$ and other rare processes ΔM_q ($q = s, d$), $B \rightarrow X_s \gamma$, $B_s \rightarrow \mu^+ \mu^-$ and $B_q \rightarrow X_s \mu^+ \mu^-$, which are governed by the same effective Hamiltonian. It is found that regions of large $\tan \beta$ and light charged Higgs mass m_{H^\pm} can explain the measured value of $R_{K^{(*)}}$ and accommodate other B physics data as well. In contrast, the type-II two-Higgs doublet model can not.

KEYWORDS: : LHCb, Belle, type-III 2HDM, $R_{K^{(*)}}$.

Contents

1	Introduction	1
2	Yukawa sector in the Type-III 2HDM	3
2.1	Neutral scalar Yukawa couplings	3
2.2	Yukawa couplings of Charged Higgs Boson	4
3	Constraints from $B_{q''}^- \rightarrow \tau \bar{\nu}$, $B_q - \bar{B}_q$ mixing, and $\bar{B} \rightarrow X_s \gamma$	6
3.1	Limits from $B_{q''}^- \rightarrow \tau \bar{\nu}_\tau$ ($q'' = u, c$)	6
3.2	Constraints from ΔM_q	7
3.3	Constraint from the $\bar{B} \rightarrow X_s \gamma$ process	11
4	Constraints from $B_q \rightarrow \mu^+ \mu^-$ and $B_q \rightarrow X_s \mu^+ \mu^-$	12
4.1	Constraints from $B_q \rightarrow \mu^+ \mu^-$, ($q = s, d$)	12
5	Predictions of R_K and R_{K^*} in type III of 2HDM	17
6	Summary	19
A	Loop functions	20

1 Introduction

The Standard model (SM) has been completed by the discovery of the last missing piece, the Higgs boson, at the Large Hadron Collider (LHC) at CERN [1, 2]. Up to now, significant direct evidence for new physics beyond the SM need to be found at LHC with high luminosity option. Nevertheless, CMS and LHCb collaborations have presented the analysis for the rare processes like $B \rightarrow K^* \mu^+ \mu^-$, $B_s \rightarrow \mu^+ \mu^-$ and $R_{K^{(*)}} = BR(B \rightarrow K^{(*)} \mu^+ \mu^-) / BR(B \rightarrow K^{(*)} e^+ e^-)$ based on the full set Run-1 data sets. Such precision measurements can serve as a guideline in the exploration of possible new physics.

A deviations from the SM predictions [3] reported by LHCb [4, 5] and CMS [6], later confirmed by Belle [7] has shown in the rare process $B \rightarrow K^* \mu^+ \mu^-$, mainly in an angular observable called P'_5 [8] with a significance of 2–3 σ depending on the assumptions of hadronic uncertainties [9–11]. Also a 3.5 σ discrepancy in the decay $B_s \rightarrow \phi \mu^+ \mu^-$ [12] has been reported by the LHCb collaboration, where the SM prediction are based on lattice QCD computation [13, 14] and the light-cone sum rules [15]. Furthermore, a violation of lepton flavour universality has been observed by the LHCb collaborations [16], to be precise, $R_K = 0.745^{+0.090}_{-0.074} \pm 0.036$, in the range $1 \text{ GeV}^2 < q^2 < 6 \text{ GeV}^2$, and $R_{K^*}^{low} = 0.660^{+0.110}_{-0.070} \pm 0.024$, in the range $0.045 \text{ GeV}^2 < q^2 < 1.1 \text{ GeV}^2$ which deviates

by 2.6σ and 2.1σ from the SM precision prediction $R_{K^{(*)}}^{\text{SM}} = 1.0003(0.99) \pm 0.0001$, respectively [17]. When these anomalies are combined with other observables for the rare processes $b \rightarrow s\mu^+\mu^-$ transitions, it is found that a scenario with NP in C_9^μ (but not in C_9^e) is preferred. The best fit yielded a central value $C_9^\mu \sim -1$, which deviates from the prediction of the SM by 4.3σ [18, 19]. In contrast, the Wilsonian coefficient C_{10}^μ agrees with the prediction of the SM, which can be determined to a remarkable precision by the well measured quantity $\text{BR}(B_s \rightarrow \mu^+\mu^-)$.

New physics are introduced to explain these anomalies observed in $b \rightarrow s$ rare transitions. For example, by introducing new operators in the effective Hamiltonian, model independent fits [8, 10, 20, 21] have been considered. It is found that the NP operators in the form $(\bar{s}\gamma_\mu P_L b)(\bar{\ell}\gamma^\mu P_L \ell)$ can be consistent with the explanations for the $B \rightarrow K^{(*)}\mu^-\mu^+$ angular distributions measured by the LHCb collaboration. Z' models are considered in Refs. [22–32] and leptoquark models are examined in Refs. [33, 34]. Furthermore, it has been argued that as the violation of lepton flavour universality violation in R_K as well as in B decays [35] might be linked to neutrino oscillations [36].

In this work, we will explore these anomalies in the context of type III Two-Higgs Doublet model (2HDM). There are several studies on $B \rightarrow K^{(*)}\mu^-\mu^+$ in the type II 2HDM [37–40] and it was found that the type-II 2HDM could not explain the anomaly of $R_{K^{(*)}}$ in the current world average.

As a minimal extension of the SM scalar sector, the scalar spectrum of 2HDM (consists of two charged Higgs H^\pm , one CP-odd A , and two CP-even h and H (one of them can be identified as SM-like Higgs boson found at the LHC)). This model can accommodate the electroweak test precision data, B physics data, and Higgs data as well. Complementary to direct searches, indirect constraints on the general 2HDM could be obtained from the rare FCNC decays, since Higgs bosons in this model can affect these processes through the penguin and box diagrams. Typically, the most general version of 2HDM has non-diagonal fermionic couplings in flavor space, and can therefore generate tree-level flavor-changing neutral current (FCNC) phenomena, which might be inconsistent with observed data. Several ways to suppress FCNCs have been suggested in the literature. The simplest one is to impose Z_2 symmetry which forbid unwanted non-diagonal terms. Depending on the Z_2 charge assignments to the scalars and fermions, it results in four types of 2HDMs (types, I, II, X, Y)[41]. An alternative solution is to assume the so-called Cheng-Sher ansatz in the fermion sector which force the non-diagonal Yukawa couplings to proportional to the mass of the involved fermions, i.e $Y_{ij} \propto \sqrt{m_i m_j}/v$, which is called Type-III 2HDM [43]. In this scenario, the absence of tree-level FCNCs is automatically guaranteed by assuming the alignment in flavor space of the Yukawa matrices. In this work, the type-III 2HDM will be carefully examined. We find the parameter region with large $\tan\beta$ (say $30 < \tan\beta < 50$) and light charged Higgs boson (say $150 \text{ GeV} < m_{h^\pm} < 350 \text{ GeV}$) can offer an explanation to the measured R_K value and accommodate pretty well the other B physics data, like ΔM_q ($q = s, d$), $B \rightarrow X_s\gamma$, $B_q \rightarrow \mu^+\mu^-$, and $B_q \rightarrow X_s\mu^+\mu^-$.

The paper is organized as follows: In section 2, we review the Yukawa sector in the type-III 2HDM. In section 3 we study constraints from $B_{q''}^- \rightarrow \tau\bar{\nu}$, $B_q - \bar{B}_q$ mixing, and $\bar{B} \rightarrow X_s\gamma$ followed by constraints from $B_q \rightarrow \mu^+\mu^-$ and $\bar{B}_q \rightarrow X_s\mu^+\mu^-$ in section 4. In

section 5, we examine the results of R_K and $R_{K^{(*)}}$ in type III of 2HDM. In section 6 we summarize our studies.

2 Yukawa sector in the Type-III 2HDM

In this section, we briefly describe the Yukawa sector of the type-III 2HDM. In order to derive the scalar Yukawa couplings to the SM quarks and leptons, we put the Higgs doublets Φ_1 and Φ_2 as:

$$\Phi_i = \begin{pmatrix} \omega_i^+ \\ \frac{1}{\sqrt{2}}(v_i + h_i + iz_i) \end{pmatrix}, \quad (2.1)$$

where there are eight scalar fields, $v_{1(2)}$ is the vacuum expectation value (VEV) of $\Phi_{1(2)}$, which is related to the W -boson mass as $m_W = gv/2$ with $v = \sqrt{v_1^2 + v_2^2} \approx 246$ GeV (g being the $SU(2)_L$ gauge coupling). After the spontaneous symmetry breaking $SU(2)_L \times U(1)_Y \rightarrow U(1)_{em}$, three of eight scalar fields become pseudo-Nambu-Goldstone bosons. The remaining five scalar fields are physical states, which include two charged-Higgs (H^\pm), one CP-odd pseudoscalar (A), and two CP-even scalars (H, h). Accordingly, the physical and weak eigenstates can be expressed as:

$$\begin{pmatrix} h_1 \\ h_2 \end{pmatrix} = R(\alpha) \begin{pmatrix} H \\ h \end{pmatrix}, \quad \begin{pmatrix} z_1 \\ z_2 \end{pmatrix} = R(\beta) \begin{pmatrix} z \\ A \end{pmatrix}, \quad \begin{pmatrix} \omega_1^+ \\ \omega_2^+ \end{pmatrix} = R(\beta) \begin{pmatrix} \omega^+ \\ H^+ \end{pmatrix}, \quad (2.2)$$

where angle α denotes the mixing between the two CP-even H and h ; angle β is defined by $\cos \beta(\sin \beta) = v_{1(2)}/v$; z and ω^\pm denote the Nambu-Goldstone bosons, and the three rotating matrices can be unified as:

$$R(\theta) = \begin{pmatrix} \cos \theta & -\sin \theta \\ \sin \theta & \cos \theta \end{pmatrix}. \quad (2.3)$$

For the purpose of phenomenological study, it is convenient to set $\sin(\beta - \alpha) = 1$.

2.1 Neutral scalar Yukawa couplings

In the type-III 2HDM, the Yukawa couplings to the quarks and leptons can be written as:

$$-\mathcal{L}_Y = \bar{Q}_L(Y_1^d \Phi_1 + Y_2^d \Phi_2)d_R + \bar{Q}_L(Y_1^u \tilde{\Phi}_1 + Y_2^u \tilde{\Phi}_2)u_R + \bar{L}_L(Y_1^\ell \Phi_1 + Y_2^\ell \Phi_2)e_R + \text{H.c.}, \quad (2.4)$$

where the flavor indices are suppressed; $\tilde{\Phi}_i = i\sigma_2 \Phi_i^*$ and σ_2 is the Pauli matrix; $Q_L(L_L)$ denotes the left-handed doublet quarks (leptons); u_R , d_R , and e_R are the right-handed up-type quarks, down-type quarks, and charged-leptons, respectively, and Y_i^f are the 3×3 complex Yukawa matrices in flavor space. Using Eq. (2.1), the fermion mass matrix can be formulated as:

$$-\mathcal{L}_Y \supset \bar{f}_L \mathbf{M}^f f_R + \text{H.c.} \equiv \bar{f}_L \left(\frac{v_1 Y_1^f}{\sqrt{2}} + \frac{v_2 Y_2^f}{\sqrt{2}} \right) f_R + \text{H.c.} \quad (2.5)$$

Without assuming the relation between Y_1^f and Y_2^f , in general, both Yukawa matrices cannot be simultaneously diagonalized which leads to the flavor-changing neutral currents (FCNCs) mediated by scalar bosons at the tree level.

To diagonal fermion mass matrix, we introduce the unitary matrices U_L^f and U_R^f , where the physical and weak states are related by $f_L^p = U_L^f f_L^w$ and $f_R^p = U_R^f f_R^w$. Thus, the couplings of neutral scalars to quarks can be expressed as:

$$\begin{aligned} -\mathcal{L}_Y^\phi = & \bar{u}_L \left[\left(\frac{c_\alpha \mathbf{m}^u}{vs_\beta} - \frac{c_{\beta-\alpha} \Xi^u}{\sqrt{2}s_\beta} \right) h + \left(\frac{s_\alpha \mathbf{m}^u}{s_\beta v} + \frac{s_{\beta-\alpha} \Xi^u}{\sqrt{2}s_\beta} \right) H \right] u_R \\ & + \bar{d}_L \left[\left(-\frac{s_\alpha \mathbf{m}^d}{vc_\beta} + \frac{c_{\beta-\alpha} \Xi^d}{\sqrt{2}c_\beta} \right) h + \left(\frac{c_\alpha \mathbf{m}^d}{c_\beta v} - \frac{s_{\beta-\alpha} \Xi^d}{\sqrt{2}c_\beta} \right) H \right] d_R \\ & - i \left[\bar{u}_L \left(\frac{\mathbf{m}^u}{t_\beta v} - \frac{\Xi^u}{\sqrt{2}s_\beta} \right) u_R + \bar{d}_L \left(\frac{t_\beta \mathbf{m}^d}{v} - \frac{\Xi^d}{\sqrt{2}c_\beta} \right) d_R \right] A + H.c., \end{aligned} \quad (2.6)$$

where $\mathbf{m}^f = U_L^f \mathbf{M}^f U_R^{f\dagger}$ denotes the diagonal mass matrix, $\Xi^u = U_L^u Y_1^u U_R^{u\dagger}$, $\Xi^d = U_L^d Y_2^d U_R^{d\dagger}$, $c_\alpha(s_\alpha) = \cos \alpha(\sin \alpha)$, $c_\beta(s_\beta) = \cos \beta(\sin \beta)$, $c_{\beta-\alpha}[s_{\beta-\alpha}] = \cos(\beta - \alpha)[\sin(\beta - \alpha)]$, and $t_\beta = \tan \beta$. We note that the couplings of the charged-leptons can be obtained in a straightforward way when \mathbf{m}^d , Y_2^d , and $U_{L,R}^d$ are replaced by \mathbf{m}^ℓ , Y_2^ℓ , and $U_{L,R}^\ell$, respectively. From Eq. (2.6), it is noticed that tree-level FCNC processes are associated with non-vanishing Ξ^u , Ξ^d , and Ξ^ℓ ; and when they vanish, it can be realized either by imposing the alignment of the two Yukawa matrices, the Yukawa interactions are returned to the type-II 2HDM.

In order to naturally suppress the FCNCs at the tree level, we adopt the so-called Cheng-Sher ansatz [43] in the quark and lepton sectors, where Ξ^f is parameterized as $\Xi_{ij}^f = \sqrt{m_i^f m_j^f} \chi_{ij}^f / v$, and χ_{ij}^f are taken as dimensionless free parameters. Although in general $\chi_{ij}^f \neq \chi_{ji}^f$ with $i \neq j$, to simplify the numerical analysis, we assume $\chi_{ij}^f = \chi_{ji}^f$ in our analysis. Thus, the neutral scalar Yukawa couplings to the quarks and leptons can be generally written as:

$$-\mathcal{L}_Y^\phi = \sum_{f=u,d,\ell} \frac{m_j^f}{v} \left[(\xi_h^f)_{ij} \bar{f}_{Li} f_{Rj} h + (\xi_H^f)_{ij} \bar{f}_{Li} f_{Rj} H - i(\xi_A^f)_{ij} \bar{f}_{Li} f_{Rj} A \right] + H.c., \quad (2.7)$$

where $(\xi_\phi^f)_{ij}$ with $\phi = h, H, A$ are given in Table 1.

2.2 Yukawa couplings of Charged Higgs Boson

The rotation matrix for charged scalars in Eq. (2.2) is the same as that for pseudoscalars; therefore, the Yukawa couplings of the charged Higgs boson are similar to those of the CP-odd scalar and can be written as:

$$\begin{aligned} \mathcal{L}_Y^{H^\pm} = & \frac{\sqrt{2}}{v} \bar{u}_i \left(m_i^u (\xi_A^{u*})_{ki} V_{kj} P_L + V_{ik} (\xi_A^d)_{kj} m_j^d P_R \right) d_j H^+ \\ & + \frac{\sqrt{2}}{v} \bar{\nu}_i (\xi_A^\ell)_{ij} m_j^\ell P_R \ell_j H^+ + H.c., \end{aligned} \quad (2.8)$$

Table 1. Yukawa couplings of the h , H , and A bosons to the quarks and leptons in type-III 2HDM. The couplings in type-II 2HDM can be easily obtained when χ_{ij}^f vanish.

ϕ	$(\xi_\phi^u)_{ij}$	$(\xi_\phi^d)_{ij}$	$(\xi_\phi^\ell)_{ij}$
h	$\frac{c_\alpha}{s_\beta} \delta_{ij} - \frac{c_{\beta-\alpha}}{\sqrt{2}s_\beta} \sqrt{\frac{m_i^u}{m_j^u}} \chi_{ij}^u$	$-\frac{s_\alpha}{c_\beta} \delta_{ij} + \frac{c_{\beta-\alpha}}{\sqrt{2}c_\beta} \sqrt{\frac{m_i^d}{m_j^d}} \chi_{ij}^d$	$-\frac{s_\alpha}{c_\beta} \delta_{ij} + \frac{c_{\beta-\alpha}}{\sqrt{2}c_\beta} \sqrt{\frac{m_i^\ell}{m_j^\ell}} \chi_{ij}^\ell$
H	$\frac{s_\alpha}{s_\beta} \delta_{ij} + \frac{s_{\beta-\alpha}}{\sqrt{2}s_\beta} \sqrt{\frac{m_i^u}{m_j^u}} \chi_{ij}^u$	$\frac{c_\alpha}{c_\beta} \delta_{ij} - \frac{s_{\beta-\alpha}}{\sqrt{2}c_\beta} \sqrt{\frac{m_i^d}{m_j^d}} \chi_{ij}^d$	$\frac{c_\alpha}{c_\beta} \delta_{ij} - \frac{s_{\beta-\alpha}}{\sqrt{2}c_\beta} \sqrt{\frac{m_i^\ell}{m_j^\ell}} \chi_{ij}^\ell$
A	$\frac{1}{t_\beta} \delta_{ij} - \frac{1}{\sqrt{2}s_\beta} \sqrt{\frac{m_i^u}{m_j^u}} \chi_{ij}^u$	$t_\beta \delta_{ij} - \frac{1}{\sqrt{2}c_\beta} \sqrt{\frac{m_i^d}{m_j^d}} \chi_{ij}^d$	$t_\beta \delta_{ij} - \frac{1}{\sqrt{2}c_\beta} \sqrt{\frac{m_i^\ell}{m_j^\ell}} \chi_{ij}^\ell$

where the sum over flavor indices is indicated, $V \equiv V_L^u V_L^{d\dagger}$ is the Cabibbo-Kobayashi-Maskawa (CKM) matrix, and $P_{R,L} = (1 \pm \gamma_5)/2$ are the chiral projection operators. Since the CKM matrix elements have hierarchy properties when different generations of fermions are involved, in the following, we examine the possible enhancement factor for $\bar{u}_i b H^+$ and $\bar{u}_i s H^+$ vertices in the type-III model. For the sake of convenience, we define $C_{ij}^L = m_i^u (\xi_A^{u*})_{ki} V_{kj}$ and $C_{ij}^R = V_{ik} (\xi_A^d)_{kj} m_j^d$.

ubH^+ vertex: With $\xi_A^{u,d}$ shown in Table 1 and $t_\beta > 1$, the C_{ub}^L coupling can be simplified as:

$$C_{ub}^L = m_u \left(\frac{1}{t_\beta} - \frac{\chi_{11}^u}{\sqrt{2}s_\beta} \right) V_{ub} - \frac{\sqrt{m_u m_c} \chi_{21}^u}{\sqrt{2}s_\beta} V_{cb} - \frac{\sqrt{m_u m_t} \chi_{31}^u}{\sqrt{2}s_\beta} V_{tb} \approx -\frac{\sqrt{m_u m_t} \chi_{31}^u}{\sqrt{2}s_\beta} V_{tb}. \quad (2.9)$$

It can be seen that due to $O(\sqrt{m_u m_t}/v) \sim V_{ub}$, unless $\chi_{31}^u \ll 1$, C_{ub}^L can have a sizable effect on the $b \rightarrow u$ decay, where the one in type-II is negligible. The situations in C_{ub}^R are different from C_{ub}^L . If we decompose C_{ub}^R to be:

$$C_{ub}^R = -V_{ud} \frac{\sqrt{m_d m_b} \chi_{13}^d}{\sqrt{2}c_\beta} - V_{us} \frac{\sqrt{m_s m_b} \chi_{23}^d}{\sqrt{2}c_\beta} + V_{ub} m_b \left(t_\beta - \frac{\chi_{33}^d}{\sqrt{2}c_\beta} \right), \quad (2.10)$$

it can be seen that due to $V_{ud} \sqrt{m_d m_b} \sim V_{us} \sqrt{m_s m_b} \gg V_{ub} m_b$, the first two terms in Eq. (2.10) are compatible and cannot be neglected. However, if we further assume $\chi_{13,23}^d \ll 0.1$, we then have $C_{ub}^R \approx V_{ub} (\xi_A^d)_{33} m_b$, which is similar to the coupling in the type-II case.

$c(t)bH^+$ vertex: Following the above discussions for the ubH^+ coupling, the C_{cb}^L coupling can be expressed as:

$$C_{cb}^L = m_c (\xi_A^{u*})_{12} V_{ub} + m_c (\xi_A^{u*})_{22} V_{cb} + m_c (\xi_A^{u*})_{32} V_{tb} \approx -\frac{\sqrt{m_c m_t}}{\sqrt{2}s_\beta} \chi_{32}^u V_{tb}, \quad (2.11)$$

where $V_{tb} \gg V_{cb} \gg V_{ub}$ is used. It is of interest to numerically see $\sqrt{m_c m_t}/v \sim V_{cb}$; that is, if χ_{32}^u or χ_{tc}^u is of $O(1)$, the charged-Higgs effect C_{cb}^L will significantly enhance the $b \rightarrow c$ decays. Based on the fact that $|V_{cd}| \sqrt{m_d m_b} \ll V_{cs} \sqrt{m_s m_b}$ and $V_{cb} m_b$, C_{cb}^R can be written as:

$$C_{cb}^R \approx -V_{cs} \frac{\sqrt{m_s m_b} \chi_{23}^d}{\sqrt{2}c_\beta} + V_{cb} m_b \left(t_\beta - \frac{\chi_{33}^d}{\sqrt{2}c_\beta} \right), \quad (2.12)$$

where due to $V_{cb}m_b < V_{cs}\sqrt{m_s m_b}$, the first term in C_{cb}^R cannot be neglected except if $\chi_{23}^d \ll 0.1$. Since t - b - H^+ couplings are normally associated with large CKM matrix element with $V_{tb} \approx 1$, therefore, they can be expressed as: $C_{tb}^L \approx m_t(\xi_A^{u*})_{33}V_{tb}$ and $C_{tb}^R \approx V_{tb}(\xi_A^d)_{33}m_b$. $u(c)sH^+$ vertex: To analyze the $u(c)$ - s - H^+ couplings, it is convenient to include the factor $\sqrt{2}/v$. Thus, $C_{us}^{L,R}$ and $C_{cs}^{L,R}$ can be reduced to be:

$$\begin{aligned}\frac{\sqrt{2}}{v}C_{us}^L &\approx -\frac{\sqrt{m_u m_c}}{s_\beta v}\chi_{21}^u V_{cs} - \frac{\sqrt{m_u m_t}}{s_\beta v}\chi_{31}^u V_{ts} \ll 1 \quad (\text{negligibly}) \\ \frac{\sqrt{2}}{v}C_{cs}^L &\approx \frac{\sqrt{2}m_c}{v}(\xi_A^{u*})_{22}V_{cs} - \frac{\sqrt{m_c m_t}}{s_\beta v}\chi_{32}^u V_{ts} \ll 1 \quad (\text{negligibly}) \\ \frac{\sqrt{2}}{v}\frac{C_{us}^R}{V_{us}} &\approx \frac{\sqrt{2}}{v}\frac{C_{cs}^R}{V_{cs}} \approx \frac{\sqrt{2}m_s}{v}\left(t_\beta - \frac{\chi_{22}^d}{\sqrt{2}c_\beta}\right).\end{aligned}\quad (2.13)$$

Although $m_s/v \sim 3.9 \times 10^{-4}$ in $C_{us,cs}^R/v$ is a suppression factor, due to an enhancement from a large t_β or $1/c_\beta$, $u(c)$ - s - H^\pm coupling can reach a few percent level. Since there is no other enhancement factor in $C_{us(cs)}^L$, their couplings are below 1% and can be neglected. tsH^+ vertex: $m_t V_{ts} \sim 6.72 \text{ GeV} < \sqrt{m_c m_t} V_{cs} \sim 14.8 \text{ GeV}$, $m_s V_{ts} \ll \sqrt{m_s m_b} V_{tb} \sim 0.66 \text{ GeV}$, we can simplify $C_{ts}^{L,R}$ to be:

$$\begin{aligned}C_{ts}^L &\approx -\frac{\sqrt{m_c m_t}}{\sqrt{2}s_\beta}\chi_{23}^u V_{cs} + m_t\left(\frac{1}{t_\beta} - \frac{\chi_{33}^u}{\sqrt{2}s_\beta}\right)V_{ts}, \\ C_{ts}^R &\approx -V_{tb}\frac{\sqrt{m_s m_b}}{\sqrt{2}s_\beta}\chi_{32}^d.\end{aligned}\quad (2.14)$$

If $\chi_{23}^u > \chi_{33}^u$, numerically, we can drop the second term in C_{ts}^L , which only involves χ_{23}^u .

3 Constraints from $B_{q''}^- \rightarrow \tau \bar{\nu}$, $B_q - \bar{B}_q$ mixing, and $\bar{B} \rightarrow X_s \gamma$

From the discussions in section.2, the essential ingredients in the Yukawa sector especially the couplings of the charged Higgs scalars to quarks and leptons are extracted. Obviously, the new free parameters are associated to the masses of quarks in the leading contributions. Consequently, we argued that the lightest charged Higgs with the new couplings might have interesting phenomenologies in some rare decays which are suppressed in the SM. Hence, in the following analysis, we will focus on the contributions of charged Higgs boson as well as neutral Higgs bosons to the relevant FCNC processes of B mesons.

3.1 Limits from $B_{q''}^- \rightarrow \tau \bar{\nu}_\tau$ ($q'' = u, c$)

As emphasized in section.2, we know that a CKM suppression charged-Higgs coupling in type-II model can be turned to a CKM enhancement coupling in type-III model. Since the CKM matrix elements are well measured in experiments, a rare decay process may give a stringent constraint on the $\chi_{ij}^{u,d}$ new parameters when a large CKM is involved in the interaction vertex. To understand the constraints, we consider the $B_{u(c)} \rightarrow \tau \bar{\nu}_\tau$ decays, where the branching ratio (BR) for $B_u \rightarrow \tau \bar{\nu}_\tau$ averaged by heavy flavor averaging group

(HFAG) is $BR(B_u \rightarrow \tau \bar{\nu}_\tau) = (1.06 \pm 0.19) \times 10^{-4}$. Although $B_c \rightarrow \tau \bar{\nu}_\tau$ has not yet been observed, using the difference in B_c lifetime between the SM and experimental results, the upper limit is obtained as $BR(B_c \rightarrow \tau \bar{\nu}_\tau) < 30\%$ [44]. From Eqs. (2.9),(2.10),(2.11), and (2.12), it can be seen that each interaction vertex may involve several parameters; in order to understand the effects of each parameter, when we focus on one term in $C_{q''b}^{L(R)}$, we will turn off the contributions from the others if the vertex consists of one more different Yukawa coupling. In addition, the charged-Higgs couplings to the leptons also involve new free parameters χ_{ij}^ℓ , which are completely independent of $\chi_{ij}^{u(d)}$; Thus, the charged-Higgs couplings used in this section are expressed as:

$$\mathcal{L}_Y^{H^\pm} \supset \frac{\sqrt{2}}{v} \bar{q}'' [(C_{q''b}^L P_L + C_{q''b}^R P_R) b + m_\tau t_\beta \bar{\nu}_\tau P_R \tau] H^\pm + H.c., \quad (3.1)$$

where $C_{q''b}^{L,R}$ can be found from Eqs. (2.9-2.12). Accordingly, the BR for $B_{q''} \rightarrow \tau \bar{\nu}_\tau$ can be given as:

$$BR(B_{q''} \rightarrow \tau \bar{\nu}_\tau) = BR^{\text{SM}}(B_{q''} \rightarrow \tau \bar{\nu}_\tau) \left| 1 - \frac{(C_{q''b}^R - C_{q''b}^L) m_{B_{q''}}^2 t_\beta}{V_{q''b} (m_{q''} + m_b) m_{H^\pm}^2} \right|^2, \quad (3.2)$$

$$BR^{\text{SM}}(B_{q''} \rightarrow \tau \bar{\nu}_\tau) = \frac{G_F^2 |V_{q''b}|^2}{8\pi} f_{B_{q''}}^2 m_{B_{q''}} m_\tau^2 \left(1 - \frac{m_\tau^2}{m_{B_{q''}}^2} \right)^2.$$

Using $V_{ub} \approx 3.72 \times 10^{-3} e^{-i\gamma}$ with $\gamma \approx 70^\circ$, $V_{cb} \approx 0.04$ [45], $m_{B_{u(c)}} \approx 5.28(6.27)$ GeV, $f_{B_u} = 0.191$ GeV [46], and $f_{B_c} = 0.434$ GeV [47], we obtain $BR^{\text{SM}}(B_u \rightarrow \tau \bar{\nu}_\tau) = 0.89 \times 10^{-4}$ and $BR^{\text{SM}}(B_c \rightarrow \tau \bar{\nu}_\tau) \approx 0.02$. Since $BR^{\text{exp}}(B_u \rightarrow \tau \bar{\nu}_\tau)/BR^{\text{SM}}(B_u \rightarrow \tau \bar{\nu}_\tau) \sim 1.19$, if the new physics effect is required to be smaller than the SM contribution and to be within 1σ errors of data, the free parameter can be limited as:

$$|\delta_{q''}^{NP}| = \left| \frac{(C_{q''b}^R - C_{q''b}^L) m_{B_{q''}}^2 t_\beta}{V_{q''b} (m_{q''} + m_b) m_{H^\pm}^2} \right| \leq \begin{cases} 0.1 & (q'' = u), \\ 4.0 & (q'' = c). \end{cases}, \quad (3.3)$$

where the $|\delta_c^{NP}|$ upper bound is from the result of $BR(B_c \rightarrow \tau \bar{\nu}_\tau) < 30\%$. Accordingly, we show $|\delta_u^{NP}|$ in the $(\chi_{23}^d, \chi_{33}^d)$ in left plot of Fig. 1, where we assume χ_{31}^u is less than 1% through the $B_u \rightarrow \tau \bar{\nu}_\tau$ measurement. Since the upper bound from the $B_c \rightarrow \tau \bar{\nu}_\tau$ decay is still much larger than the SM result, χ_{32}^u can still be of $O(1)$. In the right panel of Fig. 1 we show the allowed regions in the $(\chi_{23}^d, \tan \beta)$ plane, as it can be seen large $\tan \beta$ is preferred when $\chi_{33,23}^d \sim O(1)$. In both plots, we use $m_{H^\pm} = 200$ GeV.

3.2 Constraints from ΔM_q

Let us now consider the bounds from the $\Delta B = 2$ processes. It is known that the tree-level FCNCs can be induced by the generic 2HDM, therefore, the measured ΔM_q ($q = d, s$) usually gives a strict limit on the parameters Ξ_{ij}^q . However, due to the suppression of $\sqrt{m_i^q m_j^q}/v$ from the Cheng-Sher ansatz, $\Delta B = 2$ processes mediated by the neutral scalars at the tree level are small and negligible. Therefore, the main contributions to the $\Delta B = 2$ processes in this study are still from the box diagrams, which arise from the W^\pm and

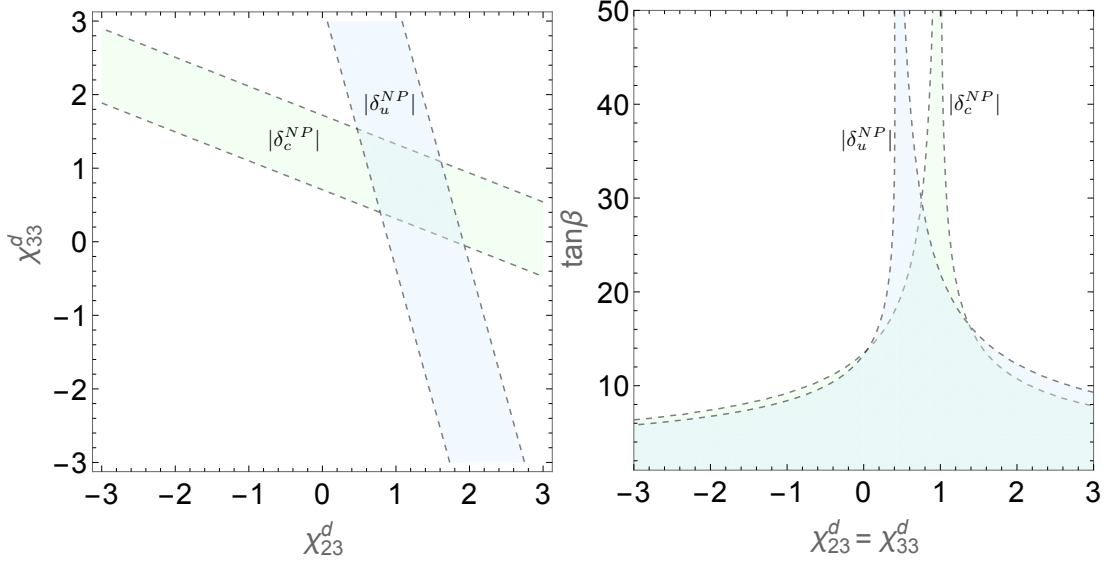


Figure 1. Allowed ranges of $|\delta_u^{NP}|$ (light green) and $|\delta_c^{NP}|$ (light blue) in the $(\chi_{23}^d, \chi_{33}^d)$ (left) and $(\chi_{23}^d, \tan \beta)$ (right) planes, We use $m_{H^\pm} = 200$ GeV in both plots.

H^\pm bosons, where the typical Feynman diagrams in 2HDM mediated by $W^\pm - H^\mp$ and $H^\pm - H^\mp$ are sketched in Fig. 2. In addition, the Yukawa couplings of H^\pm to the quarks are proportional to the quark masses. Thus, the heavier the quarks are, the larger is the enhancement of the H^\pm effects. Hence, we only consider the top-quark loop contributions in B-meson system. The relevant charged-Higgs interactions are given as:

$$\mathcal{L}_Y^{H^\pm} \supset \frac{\sqrt{2}}{v} V_{tb} \bar{t} \left(m_t \zeta_{tt}^u P_L + m_b \zeta_{bb}^d P_R \right) b H^+ + \frac{\sqrt{2}}{v} V_{tq} \bar{t} \left(m_t \zeta_{tq}^u P_L \right) q H^+ + H.c., \quad (3.4)$$

where using the scheme $\chi_{ij}^d \approx 0$ ($i \neq j$), Eq. (2.14), and $m_q \approx 0$, the coefficients $\zeta_{ij}^{q'}$ are given as:

$$\begin{aligned} \zeta_{tt}^u &\approx \frac{1}{t_\beta} \left(1 - \frac{\chi_{33}^u}{\sqrt{2} c_\beta} \right) = \frac{z_{33}^u}{t_\beta}, \quad \zeta_{bb}^d \approx t_\beta \left(1 - \frac{\chi_{33}^d}{\sqrt{2} s_\beta} \right) = t_\beta z_{33}^d, \\ \zeta_{tq}^u &\approx \frac{1}{t_\beta} \left(1 - \frac{\chi_{33}^u}{\sqrt{2} c_\beta} - \frac{\chi_{23}^u}{\sqrt{2} c_\beta} \sqrt{\frac{m_c}{m_t}} \frac{V_{cq}}{V_{tq}} \right) = \frac{z_{23}^u}{t_\beta}. \end{aligned} \quad (3.5)$$

From Eqs. (3.4) and (3.5), it can be clearly seen that when $z_{33}^u = z_{33}^d = z_{23}^u = 1$, the type-II 2HDM is reproduced. Unlike the type-II model, $z_{33,23}^u \gg 1$ can be achieved in type-III model to compensate the suppression of $1/t_\beta$ at large values of t_β . It is of interest to mention that due to the enhancement $|V_{cq}/V_{tq}|$, the third term, which has the factor $\sqrt{m_c/m_t} V_{cq}/V_{tq} \sim 2$, in ζ_{tq}^u is not suppressed and can be comparable with the second term. These new 2HDM effects may have important impacts on the flavor physics, which

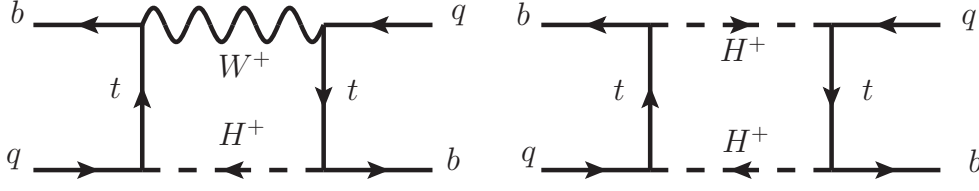


Figure 2. The sketched box diagrams for the $B_q - \bar{B}_q$ mixing mediated by the W^+ and H^+ bosons.

we want to explore in this work. Based on the conventions in [48], the effective Hamiltonian is written as:

$$H_{\text{eff}}^{\Delta B=2} = \frac{G_F^2 (V_{tb}^* V_{tq})^2}{16\pi^2} m_W^2 \sum_i C_i(\mu) Q_i, \quad (3.6)$$

where the effective operators are given as:

$$\begin{aligned} Q_1 &= (\bar{d}_L^\alpha \gamma_\mu b_L^\alpha) (\bar{d}_L^\beta \gamma^\mu b_L^\beta) \\ Q_2 &= (\bar{d}_R^\alpha b_L^\alpha) (\bar{d}_R^\beta b_L^\beta) \\ Q_3 &= (\bar{d}_R^\alpha b_L^\beta) (\bar{d}_R^\beta b_L^\alpha) \\ Q_4 &= (\bar{d}_R^\alpha b_L^\alpha) (\bar{d}_L^\beta b_R^\beta) \\ Q_5 &= (\bar{d}_R^\alpha b_L^\beta) (\bar{d}_L^\beta b_R^\alpha) \end{aligned} \quad (3.7)$$

with α, β being the color indices. The Wilson coefficients at the scale $\mu = m_b = 4.8$ GeV can be expressed as [48]:

$$C_i(m_b) \approx \sum_{k,j} \left(b_k^{(i,j)} + \eta c_k^{(i,j)} \right) \eta^{a_k} C_j(\mu_H), \quad (3.8)$$

where $\mu_H = m_{H^\pm}$, $\eta = \alpha_s(\mu_H)/\alpha_s(m_t)$, $C_j(\mu_H)$ are the Wilson coefficients at μ_H scale, and the magic numbers of $a_k^{i,j}$, $b_k^{i,j}$, and $c_k^{i,j}$ can be found in [48]. The non-vanishing Wilson coefficients at the μ_H scale induced from the WW , WH , and HH diagrams shown in Fig. 2 are $C_1(\mu_H) = C_1^{\text{SM}} + C_1^{WH} + C_1^{HH}$ and $C_2(\mu_H) = C_2^{HH}$, where the SM result is $C_1^{\text{SM}} = 4S_0(m_t^2/m_W^2) = 3.136(m_t^2/m_W^2)^{0.76} \approx 9.36$ [49], and $S_0(x)$ is the Inami-Lin function [50]. If we define $x_t = m_t^2/m_W^2$, $y_t = m_t^2/m_{H^\pm}^2$, $y_W = m_W^2/m_{H^\pm}^2$, and $y_b = m_b^2/m_{H^\pm}^2$, the results from the charged-Higgs contributions can be formulated as:

$$\begin{aligned} C_1^{WH} &= 2\zeta_{tq}^u \zeta_{tt}^{u*} y_t \left\{ \frac{y_t(4-x_t)}{(1-y_t)(y_t-y_W)} + \frac{y_W(4y_t-y_W x_t)}{(1-y_W)(y_t-y_W)^2} \ln(y_W) \right. \\ &\quad \left. - \frac{y_t y_W}{(1-y_t)^2 (y_t-y_W)^2} [(1-x_t)^2 + 3(1-x_t y_t)] \ln(y_t) \right\}, \\ C_1^{HH} &= 2x_t y_t (\zeta_{tq}^u \zeta_{tt}^{u*})^2 \left[\frac{1+y_t}{2(1-y_t)^2} + \frac{y_t \ln(y_t)}{(1-y_t)^3} \right], \\ C_2^{HH} &= 4(\zeta_{tq}^u \zeta_{bb}^{d*})^2 x_t y_t y_b \left[\frac{2}{(1-y_t)^2} + \frac{(1+y_t) \ln(y_t)}{(1-y_t)^3} \right]. \end{aligned} \quad (3.9)$$

It is of interest to see that although C_2^{HH} is proportional to the small factor y_b , due to $z_{23}^u \gg 1$ in this study, the C_2^{HH} contribution is significant. If we take $y_b = \chi_{33,23}^u = 0$, our results are the same as those obtained in [51]. Since we are interested in some what light charged-Higgs, i.e., μ_H is slightly higher than m_t , we take $\eta \approx 1$ in the numerical calculations. Thus, according to Eq. (3.8) and the magic numbers in [48], the Wilson coefficients $C_i(m_b)$ can be written as:

$$C_1(m_b) \approx 0.848C_1(\mu_H), \quad C_2(m_b) \approx 1.708C_2(\mu_H), \quad C_3(m_b) \approx -0.016C_2(\mu_H). \quad (3.10)$$

The matrix elements of the renormalized operators for $\Delta B = 2$ are defined as [48]:

$$\begin{aligned} \langle B_q | \hat{Q}_1(\mu) | \bar{B}_q \rangle &= \frac{1}{3} f_{B_q}^2 m_{B_q} B_{1q}(\mu), \\ \langle B_q | \hat{Q}_2(\mu) | \bar{B}_q \rangle &= -\frac{5}{24} \left(\frac{m_{B_q}}{m_b(\mu) + m_q(\mu)} \right)^2 f_{B_q}^2 m_{B_q} B_{2q}(\mu), \\ \langle B_q | \hat{Q}_3(\mu) | \bar{B}_q \rangle &= \frac{1}{24} \left(\frac{m_{B_q}}{m_b(\mu) + m_q(\mu)} \right)^2 f_{B_q}^2 m_{B_q} B_{3q}(\mu), \end{aligned} \quad (3.11)$$

where the operators $\hat{Q}_{1,2,3}$, quark masses, and B_{iq} parameters at m_b scale in the Landau RI-MOM scheme and the decay constants of B_q are shown in Table 2 [48, 52, 53]. Due to $B_{is} \approx B_{id}$, we will adopt $B_{is} = B_{id} = B_{iq}$ in the numerical estimations. As a result, $\langle B_q | H_{\text{eff}}^{\Delta B=2} | \bar{B}_q \rangle$ with the W^\pm - and H^\pm -boson contributions is given as:

$$\begin{aligned} \langle B_q | H_{\text{eff}}^{\Delta B=2} | \bar{B}_q \rangle &= \langle B_q | H_{\text{eff}}^{\Delta B=2} | \bar{B}_q \rangle^{\text{SM}} \left(1 + \Delta_q^{H^\pm} \right), \\ \langle B_q | H_{\text{eff}}^{\Delta B=2} | \bar{B}_q \rangle^{\text{SM}} &= \frac{G_F^2 (V_{tb}^* V_{tq})^2}{48\pi^2} m_W^2 f_{B_q}^2 m_{B_q} \hat{\eta}_{1B} B_{1q}(4S_0(x_t)), \\ \Delta_q^{H^\pm} &= \frac{1}{4S_0(x_t)} \left[C_1^{WH} + C_1^{HH} + \frac{m_{B_q}^2 C_2^{HH}}{8(m_b + m_q)^2 \hat{\eta}_{1B} B_{1q}} (-5\hat{\eta}_{2B} B_{2q} + \hat{\eta}_{3B} B_{3q}) \right] \end{aligned} \quad (3.12)$$

where $\hat{\eta}_{1B} \approx 0.848$, $\hat{\eta}_{2B} \approx 1.78$, and $\hat{\eta}_{3B} \approx -0.016$ are the QCD corrections. The mass difference between the physical B_q states can be obtained by:

$$\Delta M_q = 2 |\langle B_q | H_{\text{eff}}^{\Delta B=2} | \bar{B}_q \rangle| = \Delta M_q^{\text{SM}} |1 + \Delta_q^{H^\pm}|. \quad (3.13)$$

Taking $V_{td} \approx 0.0082e^{-i\beta}$ with $\beta \approx 22.5^\circ$, $V_{ts} \approx -0.04$, and $m_t = \bar{m}_t(m_t) \approx 165$ GeV, the B_q -meson oscillation parameters $\Delta M_{d,s}$ in the SM are respectively obtained as:

$$\begin{aligned} \Delta M_d^{\text{SM}} &\approx 3.32 \times 10^{-13} \text{ GeV} = 0.504 \text{ ps}^{-1}, \\ \Delta M_s^{\text{SM}} &\approx 1.16 \times 10^{-11} \text{ GeV} = 17.60 \text{ ps}^{-1}, \end{aligned} \quad (3.14)$$

where the current data are $\Delta M_d^{\text{exp}} = (0.5065 \pm 0.0019) \text{ ps}^{-1}$ and $\Delta M_s^{\text{exp}} = (17.756 \pm 0.021) \text{ ps}^{-1}$ [45]. In order to consider the new physics contributions, when we use the ΔM_q^{exp} to bound the free parameters, we take the SM predictions to be $\Delta M_d^{\text{SM}} = 0.555_{-0.046}^{+0.073} \text{ ps}^{-1}$ and $\Delta M_s^{\text{SM}} = 16.8_{-1.5}^{+2.6} \text{ ps}^{-1}$ [46], in which the next-to-leading order (NLO) QCD corrections [54–56] and the uncertainties from various parameters, such as CKM matrix elements,

decay constants, and top-quark mass, are taken into account. Hence, from Eq. (3.13), the bounds from $\Delta B = 2$ can be used as:

$$\begin{aligned} 0.76 &\lesssim |1 + \Delta_d^{H^\pm}| \lesssim 1.15, \\ 0.87 &\lesssim |1 + \Delta_s^{H^\pm}| \lesssim 1.38. \end{aligned} \quad (3.15)$$

Table 2. Values of quark masses and B_{iq} parameters at m_b scale in the RI-MOM scheme. The decay constants of the $B_{d,s}$ mesons are from [46].

m_b	m_s	m_q	B_{1q}	B_{2q}	B_{3q}	f_{B_s}	f_{B_d}
4.6 GeV	0.10 GeV	5.4 MeV	0.87	0.82	1.02	0.231 GeV	0.191 GeV

3.3 Constraint from the $\bar{B} \rightarrow X_s \gamma$ process

In addition to the $\Delta B = 2$ processes, the penguin induced $b \rightarrow s \gamma$ decay is also sensitive to new physics. The current experimental value is $BR(\bar{B} \rightarrow X_s \gamma)^{\text{exp}} = (3.32 \pm 0.15) \times 10^{-4}$ for $E_\gamma > 1.6$ GeV [59], and the SM prediction with next-to-next-to-leading order (NNLO) QCD corrections is $BR(\bar{B} \rightarrow X_s \gamma)^{\text{SM}} = (3.36 \pm 0.23) \times 10^{-4}$ [60, 61]. Since the SM result is close to the experimental data, $\bar{B} \rightarrow X_s \gamma$ will give a strict bound on the new physics effects.

The effective Hamiltonian arisen from the W^\pm and H^\pm bosons for $b \rightarrow s \gamma$ at μ_b scale can be written as:

$$\mathcal{H}_{b \rightarrow s \gamma} = -\frac{4G_F}{\sqrt{2}} V_{ts}^* V_{tb} (C_{7\gamma}(\mu_b) O_{7\gamma} + C_{8G}(\mu_b) O_{8G}), \quad (3.16)$$

where the electromagnetic and gluonic dipole operators are given as:

$$O_{7\gamma} = \frac{e}{16\pi^2} m_b \bar{s} \sigma^{\mu\nu} P_R b F_{\mu\nu}, \quad O_{8G} = \frac{g_s}{16\pi^2} m_b \bar{s}_\alpha \sigma^{\mu\nu} T_{\alpha\beta}^a P_R b_\beta G_{\mu\nu}^a. \quad (3.17)$$

$C_{7\gamma}(\mu_b)$ and $C_{8G}(\mu_b)$ are the Wilson coefficients at μ_b scale, and their relations to the initial conditions at the high energy scale μ_H are through renormalization group (RG) equations. The NLO [62–64] and NNLO [65] QCD corrections to the $C_{7\gamma}(\mu_b)$ and $C_{8G}(\mu_b)$ in the 2HDM have been calculated. Based on the $C_{7\gamma}^{\text{SM}}(\mu_b)$ value extracted in [66], we get $C_{7\gamma}^{\text{SM}}(\mu_b) \approx -0.304$ when $BR(\bar{B} \rightarrow X_s \gamma)^{\text{SM}} = 3.36 \times 10^{-4}$ is applied. In order to study the influence of the $b \rightarrow s \gamma$ process on the type-III model, we follow the approach in [61] and split the $BR(\bar{B} \rightarrow X_s \gamma)$ to be:

$$BR(\bar{B} \rightarrow X_s \gamma) \times 10^4 \approx (3.36 \pm 0.23) - 8.22 \text{Re}(C_{7\gamma}^{H^\pm}) - 1.99 \text{Re}(C_{8G}^{H^\pm}), \quad (3.18)$$

where $C_{7\gamma,8G}^{H^\pm}$ are the Wilson coefficients at μ_H scale, (the matching scale is $\mu_0 \sim m_t$ at which the heavy particles are decoupled [61]), and the quadratic $C_{7\gamma,8G}^{H^\pm}$ are ignored due to the requirement of $C_{7\gamma,8G}^{H^\pm} < 1$. Using the current experimental value, the bound on $C_{7\gamma,8G}^{H^\pm}$ is:

$$8.22 \text{Re}(C_{7\gamma}^{H^\pm}) + 1.99 \text{Re}(C_{8G}^{H^\pm}) \approx 0.04 \pm 0.28. \quad (3.19)$$

According to the charged-Higgs interactions in Eq. (3.4), the H^\pm contributions to $C_{7\gamma,8G}^{H^\pm}$ are expressed as [62]:

$$\begin{aligned} C_{7\gamma}^{H^\pm} &= \zeta_{tt}^u \zeta_{ts}^{u*} C_{7,LL}^{H^\pm} + \zeta_{bb}^d \zeta_{ts}^{u*} C_{7,RL}^{H^\pm}, \\ C_{8G}^{H^\pm} &= \zeta_{tt}^u \zeta_{ts}^{u*} C_{8,LL}^{H^\pm} + \zeta_{bb}^d \zeta_{ts}^{u*} C_{8,RL}^{H^\pm}, \end{aligned} \quad (3.20)$$

$$\begin{aligned} C_{7,LL}^{H^\pm} &= \frac{y_t}{72} \left[\frac{8y_t^2 + 5y_t - 7}{(1-y_t)^3} - \frac{6y_t(2-3y_t)}{(1-y_t)^4} \ln(y_t) \right], \\ C_{8,LL}^{H^\pm} &= \frac{y_t}{24} \left[\frac{y_t^2 - 5y_t - 2}{(1-y_t)^3} - \frac{6y_t}{(1-y_t)^4} \ln(y_t) \right], \\ C_{7,RL}^{H^\pm} &= \frac{y_t}{12} \left[\frac{3-5y_t}{(1-y_t)^2} + \frac{2(2-3y_t)}{(1-y_t)^3} \ln(y_t) \right], \\ C_{8,RL}^{H^\pm} &= \frac{y_t}{4} \left[\frac{3-y_t}{(1-y_t)^2} + \frac{2}{(1-y_t)^3} \ln(y_t) \right]. \end{aligned} \quad (3.21)$$

Taking $\chi_{33,23}^u = \chi_{33}^d = 0$ in Eq. (3.20), it can be found that $\zeta_{tt}^u \zeta_{ts}^{u*}$ in type-II 2HDM is suppressed by $1/t_b^2$ while the t_β -dependence in $\zeta_{bb}^d \zeta_{ts}^{u*}$ is canceled and $(\zeta_{bb}^d \zeta_{ts}^{u*})_{\text{type-II}} = 1$. As a result, the mass of charged-Higgs in type-II 2HDM has been limited to be $m_{H^\pm} > 580$ GeV at 95% confidence level (CL) by using NNLO QCD corrections [67].

In the type-III 2HDM, it is observed that in the large $\tan\beta$ region, due to the $1/c_\beta$ enhancement, the $\zeta_{bb}^d \zeta_{ts}^{u*}$ terms still dominate. Since the new parameters $\chi_{33,23}^u/c_\beta$ and χ_{33}^d/s_β are involved in Eq. (3.20), it is possible to reduce $(\zeta_{bb}^d \zeta_{ts}^{u*})_{\text{type-II}}$ far away from unity; thus, the charged-Higgs mass can be much lighter than 580 GeV which can be seen in Figure.(3) left panel. In the other hand, we can get constraints on χ_{33}^u and χ_{23}^u from the right panel of the same Figure.(3), it is clear that for $-1 \leq \chi_{33}^u \leq 0$ we obtain $-0.5 \leq \chi_{23}^u \leq 0$ and for $0 \leq \chi_{33}^u \leq 1$ the interval permitted for χ_{23}^u become $[0, 0.5]$.

4 Constraints from $B_q \rightarrow \mu^+ \mu^-$ and $B_q \rightarrow X_s \mu^+ \mu^-$

4.1 Constraints from $B_q \rightarrow \mu^+ \mu^-$, ($q = s, d$)

The effective Hamiltonian for $\Delta B = 1$ can be written as [49, 68, 69]:

$$\mathcal{H}_{eff} = -\frac{G_F}{\sqrt{2}} \alpha \left(V_{ts}^* V_{tb} \sum_i (\mathcal{C}_i \mathcal{O}_i + \mathcal{C}'_i \mathcal{O}'_i) .h.c \right), \quad (4.1)$$

Where \mathcal{C}_i and \mathcal{C}'_i are Wilson coefficients encoding the short-distance physics at the energy scale μ which is usually taken to be the b -quark mass (m_b), and can be modified from SM predictions in the presence on the new physics, while \mathcal{O}_i are the operators given by

$$\mathcal{O}_9 = (\bar{s} \gamma_\mu P_L b) (\bar{\ell} \gamma^\mu \ell), \quad \mathcal{O}_{10} = (\bar{s} \gamma_\mu P_L b) (\bar{\ell} \gamma^\mu \gamma_5 \ell), \quad (4.2)$$

$$\mathcal{O}_S = (\bar{s} P_R b) (\bar{\ell} \ell), \quad \mathcal{O}_P = (\bar{s} P_R b) (\bar{\ell} \gamma_5 \ell), \quad (4.3)$$

with $P_{L,R} = (1 \mp \gamma_5)/2$ and $m_b = m_b(\mu_b)$ denotes the running b quark mass in the \overline{MS} scheme with $\mu_b = 4.8$ GeV. The $\mathcal{O}'_{9,10}$ can be obtained from the \mathcal{O}_i by making the replacements $P_L \leftrightarrow P_R$. In the SM, three operators play an important role, namely the

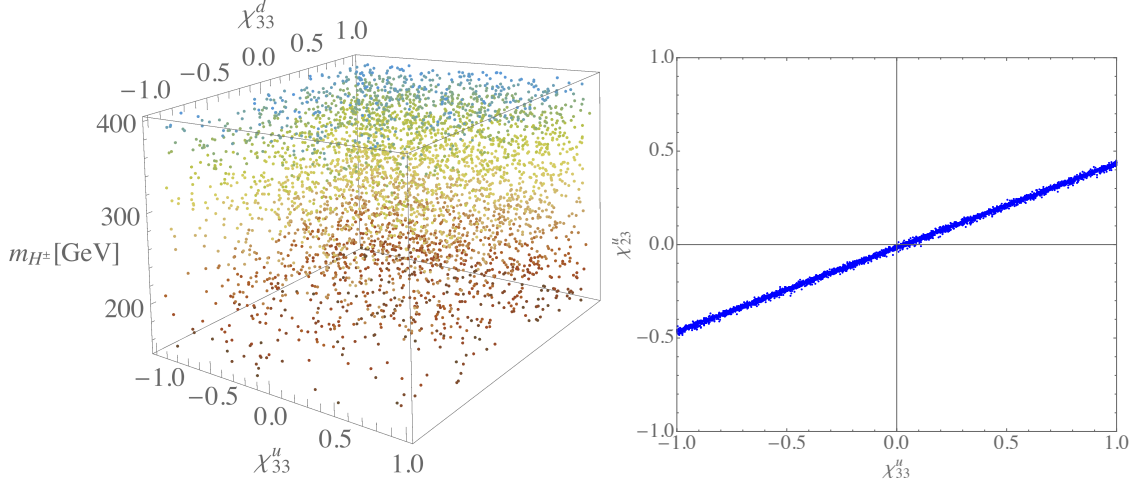


Figure 3. Left panel: allowed parameter spaces of $(m_{H^\pm}, \chi_{33}^u, \chi_{33}^d)$ with $t_\beta = [30, 60]$ when the bound from $\bar{B} \rightarrow X_s \gamma$ shown in Eq. (3.19) is satisfied. Right panel: the results of left panel project onto χ_{33}^u - χ_{33}^d plane, where $t_\beta = [30, 60]$, $m_{H^\pm} = [150, 400]$ GeV, and $\chi_{33,23}^u, \chi_{33}^d = [-3, 3]$ are included.

electromagnetic operator \mathcal{O}_7 , and the semileptonic operators $\mathcal{O}_{9,10}$, differing with respect to the chirality of the emitted charged leptons [70]. The SM values \mathcal{C}_9 and \mathcal{C}_{10} are obtained at the next-to-next-to-leading order (NNLO)[71, 74] and depend on the fundamental parameters of the top-quark mass and W -boson masses as well as the weak mixing angle θ_W . Moreover, they are universal for the three lepton flavors $\ell = e, \mu, \tau$. The other Wilson coefficients \mathcal{C}_i' are suppressed by $m_b m_\ell / m_W^2$. The Wilson coefficient in the SM are $\mathcal{C}_9 = 4.211$ and $\mathcal{C}_{10} = \mathcal{C}_{10}^{SM} = -\eta_Y Y_0(m_t^2/m_W^2)/\sin^2 \theta_W = -4.103$ [74, 75], where Y_0 is one-loop function [50] and $\eta_Y = 1.026 \pm 0.006$ summarizes the NLO corrections [50] with $m_t = \bar{m}_t(m_t)$. In the general 2HDM, $b \rightarrow s$ transition is mediated by gauge boson Z , Goldstone boson G^0 , and neutral Higgs bosons h, H and A penguin diagrams, as well as box diagrams mediated with W^\pm, H^\pm and G^\pm which lead to additional contributions to \mathcal{C}_i ($i = 7, 9, 10$) and could make the chirality-flipped operators \mathcal{O}_i ($i = 7, 9, 10$) to contribute in a significant manner through the Z - and γ diagrams shown in Fig.4. In the following we separate the contribution in two categories penguins and boxes, the scalar charged Higgs

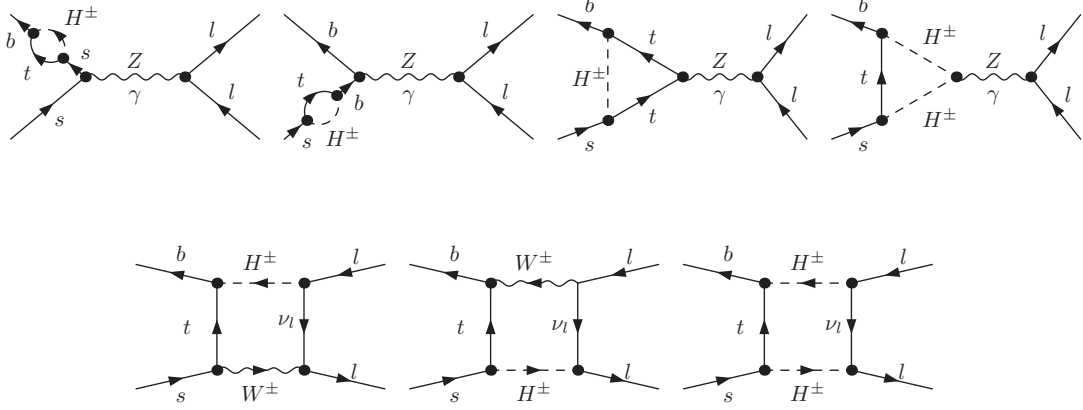


Figure 4. The sketched electroweak penguin and box diagrams for $b \rightarrow s \ell^+ \ell^-$ mediated by H^\pm and W^\pm bosons.

boson contribution comes from Z and γ -penguin are :

$$C_9 = \xi_{tt}^u \xi_{ts}^{u*} f_3(x_t, y_{H^\pm}) + \xi_{bb}^d \xi_{ts}^{u*} x_d f_4(x_t, y_{H^\pm}) + \eta_W C_{10} - 4\eta'_W \text{Re}(\xi_{tt}^u \xi_{22}^{\mu*} x_\mu f_5(x_t, y_{H^\pm})) \\ + \eta'_W \xi_{tt}^u \xi_{ts}^{u*} |\xi_{22}^\mu|^2 x_\mu f_6(x_t, y_{H^\pm}) + \eta'_W \text{Re}(\xi_{tt}^u \xi_{22}^{\mu*}) x_\mu f_7(x_t, y_{H^\pm}) \quad (4.4)$$

$$C_{10} = \eta'_W \left(\xi_{tt}^u \xi_{ts}^{u*} f_8(x_t, y_{H^\pm}) + \xi_{bb}^d \xi_{ts}^{u*} x_b f_9(x_t, y_{H^\pm}) + \xi_{tt}^u \xi_{ts}^{u*} |\xi_{22}^\mu|^2 x_\mu f_{10}(x_t, y_{H^\pm}) \right. \\ \left. + \text{Re}(\xi_{tt}^u \xi_{22}^{\mu*}) x_\mu f_{11}(x_t, y_{H^\pm}) \right) \quad (4.5)$$

$$C_P = \sqrt{x_b x_\mu} \left[\xi_{tt}^{u*} \xi_{bb}^d \eta'_W g_1(x_t, y_{H^\pm}) + \xi_{tt}^u \xi_{ts}^{u*} \left(g_2(x_t, y_{H^\pm}) - \eta'_W g_3(x_t, y_{H^\pm}) \right) \right. \\ \left. + \eta'_W \left(\xi_{22}^\mu \xi_{tt}^{u*} g_4(x_t, y_{H^\pm}) - \xi_{22}^{\mu*} \xi_{tt}^u g_5(x_t, y_{H^\pm}) - 2\xi_{bb}^d \xi_{22}^{\mu*} g_6(x_t, y_{H^\pm}) \right) \right] \quad (4.6)$$

$$C_S = \sqrt{x_b x_\mu} \eta'_W \left[\xi_{22}^\mu \xi_{tt}^{u*} g_4(x_t, y_{H^\pm}) + \xi_{22}^{\mu*} \xi_{tt}^u g_5(x_t, y_{H^\pm}) + 2\xi_{bb}^d \xi_{22}^{\mu*} g_6(x_t, y_{H^\pm}) \right] \quad (4.7)$$

where $\eta_W = (-1 + 4 \sin^2 \theta_W)$ and $\eta'_W = \sin^{-2} \theta_W$. With $x_i = m_i^2/m_W^2$ with $i = t, b, \mu$ and $y_{H^\pm} = m_{H^\pm}^2/m_W^2$. The corresponding loop functions f_i and g_i can be found in Appendix A. In what follow, we will concentrate our discussion on the Wilson coefficients C_9 and C_{10} which can be extracted from different angular observables, in particular in the case of $B \rightarrow K^* \mu^+ \mu^-$ which provides a several observables through angular study of the decay which have been experimentally studied at LHCb[76, 77], CMS[6, 78], ATLAS[79], Belle[7, 80] and BABAR [81]. Several observables have shown deviations from SM predictions. It started with the set of observables P'_5 , $Q_5 = P_5^\mu - P_5^{e'}$, forward-backward asymmetry (A_{FB}), lepton-flavour universality violating ratio R_{K^*} .

Several global fits exist for NP contributions to the Wilson coefficients $C_{9,10}$ [10, 22, 82]. These fits includes the branching ratios of $B \rightarrow K \mu^+ \mu^-$, $B \rightarrow K^* \mu^+ \mu^-$, $B_s \rightarrow \phi \mu^+ \mu^-$, $B_s \rightarrow X_s \mu^+ \mu^-$ (restricted only to the range $q^2 \in [1, 6] \text{ GeV}^2$), $B \rightarrow X_s \gamma$, $B_s \rightarrow \mu^+ \mu^-$ as well as some isospin symmetry and time-dependent CP asymmetry of $B \rightarrow K^* \gamma$. To be

more conservative, we use the central values given by:

$$C_7 = -0.017 \pm 0.030, \quad C_9 = -1.02 \pm 0.27, \quad C_{10} = 0.16 \pm 0.24, \quad (4.8)$$

and we use the following correlation coefficients $\rho_{C_7, C_9} = -0.28$ and $\rho_{C_9, C_{10}} = +0.06$. These bounds can be used to impose constraints on our parameters space. We show in Figure.(5) the correlation between Wilson coefficients in the allowed region with the same parameters as in Figure.(3) and taking into account constraints from $BR(b \rightarrow s\gamma)$ at 95% CL. As can be seen $C_9 < 0$ is preferred by data, and the possibility $C_9 = -C_{10}$ can also be a good fit.

The expression for the branching ratio $B_s \rightarrow \mu^+ \mu^-$ is given by

Table 3. Current measurement with $1 \text{ GeV}^2 < q^2 < 6 \text{ GeV}^2$.

$BR(B \rightarrow X_s \mu^+ \mu^-)[57]$	$BR(B_s \rightarrow \mu^+ \mu^-)[58]$
$(0.66^{+0.82+0.30}_{-0.76-0.24} \pm 0.07) \times 10^{-6}$	$(2.4^{+0.9}_{-0.7}) \times 10^{-9}$

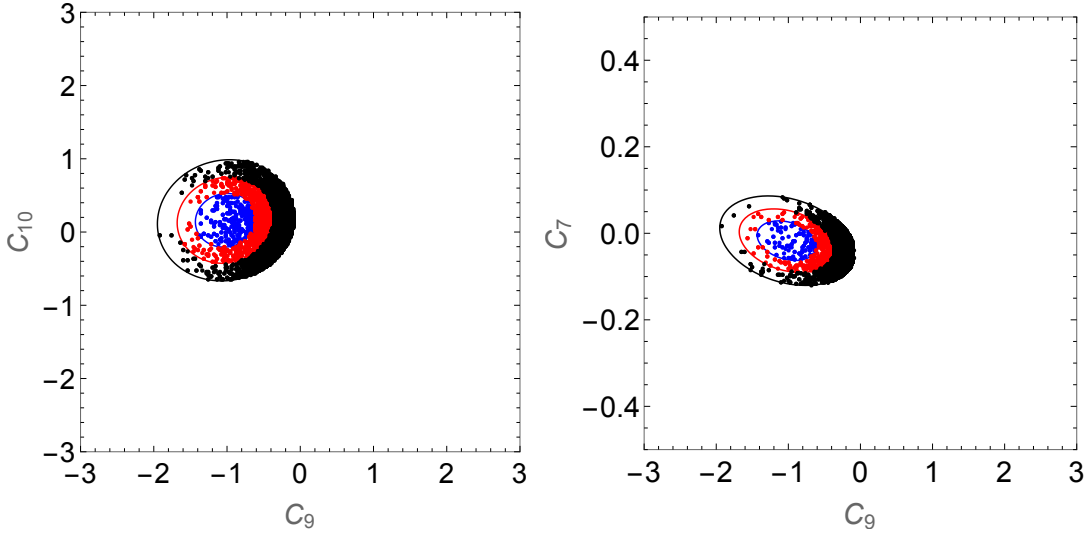


Figure 5. Correlation between Wilson coefficients in the allowed region of $BR(b \rightarrow s\gamma)$ at 95% CL and the Eq.(4.8).

$$BR(B_s \rightarrow \mu^+ \mu^-) = \tau_{B_s} m_{B_s}^3 f_{B_s}^2 m_\mu^2 \beta \frac{\alpha^2 G_F^2}{16\pi^3} |V_{tb} V_{ts}|^2 \left[\left| C_{10} + \frac{m_{B_s}^2}{2m_\ell(m_b + m_s)} C_P \right|^2 + \frac{m_{B_s}^4 \beta^2}{4m_\ell^2(m_b + m_s)^2} \left| C_S \right|^2 \right] \quad (4.9)$$

with $\beta = (1 - 4m_\mu^2/m_{B_s}^2)^{1/2}$, where C_9 does not contribute. In the above relation $BR(B_s \rightarrow \mu^+ \mu^-)$ is calculated by ignoring the $B_s - \bar{B}_s$ mixing. Experiments measure the average time-integrated branching ratio denoted by $\overline{BR}(B_s \rightarrow \mu^+ \mu^-)$ and the two are related as

$\overline{BR}(B_s \rightarrow \mu^+\mu^-) = \frac{1+y_s\Delta A_s}{1-y_s^2} BR(B_s \rightarrow \mu^+\mu^-)$. Where $y_s = 0.062 \pm 0.006$ [45, 59, 83] and ΔA_s is the CP asymmetry due to vanishing width difference, which is $\Delta A_s = +1$ in the SM, but in general it can be $\Delta A_s \in [-1, 1]$ [84]. The SM prediction of the branching ratio of a B_s meson decaying into two muons is calculated to be $\overline{BR}(B_s \rightarrow \mu^+\mu^-)_{SM} = (3.66 \pm 0.23) \times 10^{-9}$. This prediction is particularly precise thanks to the purely leptonic final state which reduce the dependence on computations of the strong force. A fit to the invariant mass of the dimuon candidates $m_{\mu\mu}$ have been performed by LHCb and CMS groups. The measured Branching ratio is given in Table.3 with 6.2 standard deviations. In order to probe new physics effects, it's convenient to define the quantity R_{B_s} by

$$R_{B_s} = \frac{\overline{BR}(B_s \rightarrow \mu^+\mu^-)}{\overline{BR}(B_s \rightarrow \mu^+\mu^-)_{SM}} = |P|^2 + |S|^2 \quad (4.10)$$

where S and P are given by[72]

$$P = \frac{C_{10}}{C_{10}^{SM}} + \frac{m_{B_s}^2}{2m_\mu(m_b + m_s)} \frac{C_P}{C_{10}^{SM}} \quad \text{and} \quad S = \frac{m_{B_s}^2\beta}{2m_\mu(m_b + m_s)} \frac{C_S}{C_{10}^{SM}} \quad (4.11)$$

In the SM, $C_{10} = C_{10}^{SM}$, then $P_{SM} = 1$ and $S_{SM} = 0$. Combining the experimental values we get: $R_{B_s} = 0.90_{-0.34}^{+0.42}$. Although the uncertainty in this ratio is somewhat large, values smaller than unity seem to be preferred. In type-II 2HDM, the C_S and C_P contributions to Eq.(4.11) are suppressed [73] unless for large Yukawa couplings, however in type-III 2HDM, it gets large enhancements from the $\xi_{tt,bb}^{u,d}$ parameters, where the contribution depends also on m_{H^\pm} and $\tan\beta$.

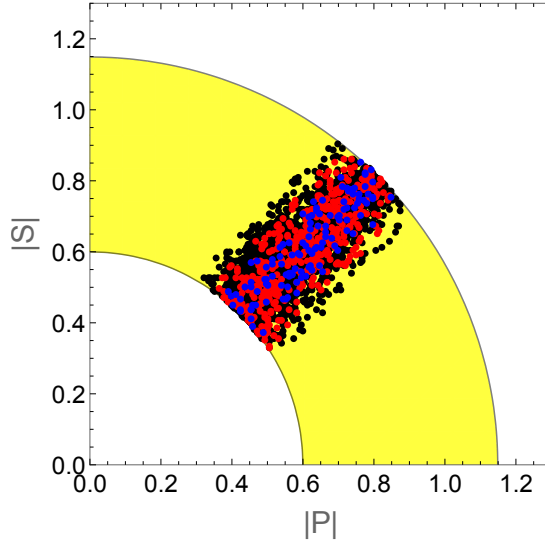


Figure 6. Correlations between Wilson coefficients P and S . Taking into account constraints from Eq. (4.8) as well as from $BR(b \rightarrow s\gamma)$. Yellow band represent 2σ of R_{B_s} .

Other complementary information on Wilson coefficients can be extracted from the decay $B_q \rightarrow X_s \mu^+ \mu^-$ branching ratios in the range $1 \text{ GeV}^2 < q^2 = m_{\mu\mu}^2 < 6 \text{ GeV}^2$. We

use the integrated rate as given in Ref [74]:

$$\begin{aligned}
BR(B_q \rightarrow X_s \mu^+ \mu^-) = & \left(2.1913 - 0.001655\mathcal{I}(r_{10}) + 0.0535\mathcal{I}(r_7) + 0.00496\mathcal{I}(r_7 r_9^*) \right. \\
& - 0.0118\mathcal{I}(r_9) - 0.5426\mathcal{R}(r_{10}) + 0.0281\mathcal{R}(r_7) + 0.0153\mathcal{I}(r_{10}^* r_7) \\
& - 0.8554\mathcal{I}(r_7 r_9^*) + 2.7008\mathcal{R}(r_9) - 0.10705\mathcal{I}(r_9 r_{10}^*) + 10.7687|r_{10}|^2 \\
& \left. + 0.2889|r_7|^2 + 1.4882|r_9|^2 \right) \times 10^{-7}
\end{aligned} \tag{4.12}$$

where $r_i = C_i/C_i^{SM}$. The SM predictions is $BR(B_q \rightarrow X_s \mu^+ \mu^-) = (1.59 \pm 0.11) \times 10^{-6}$.

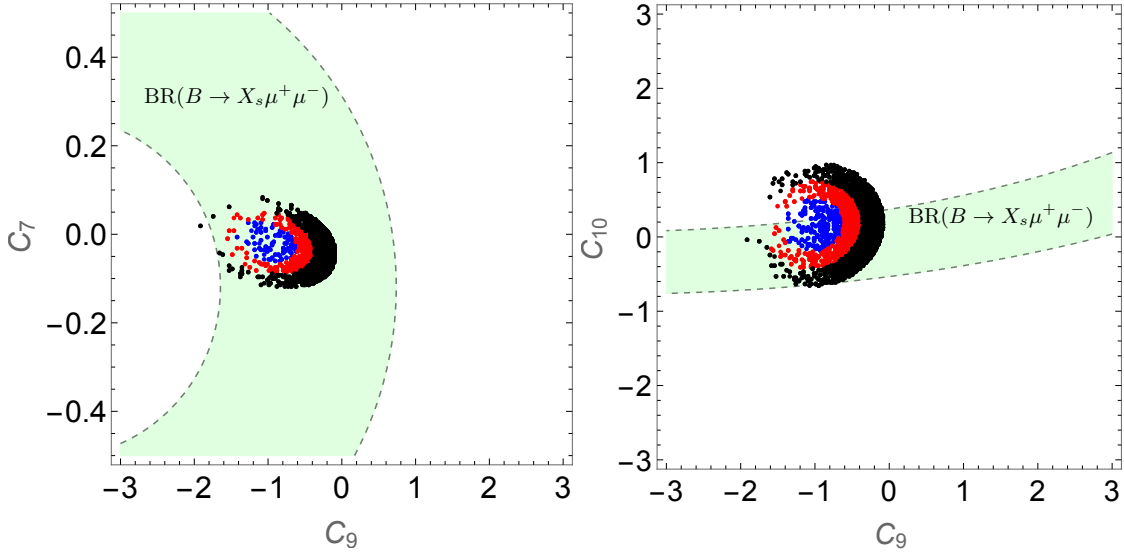


Figure 7. 90%CL bounds in the (C_9, C_{10}) (left) and (C_9, C_7) (right) planes following the experimental branching ratio of $BR(B_q \rightarrow X_s \mu^+ \mu^-)$. The scatter points correspond to expectation in type-III-2HDM.

We impose the experimental bound on $BR(B \rightarrow X_s \mu^+ \mu^-)$ at 90%CL and include constraints from Eq.(4.8). We present in Fig.7 the resulting allowed scatter points in the (C_9, C_{10}) (left) plane with $C_7 = -0.017$ and $C_{10} = 0.16$ in the right plot. The regions in Fig.7 suggest that the best fit to data is achieved if non-zero contributions are present for $C_{7,9,10}$ Wilson coefficient that involve muons and those $C_{7,9,10} \neq 0$ seem to be preferred.

5 Predictions of R_K and R_{K^*} in type III of 2HDM

In terms of the operators of the type (4.3).The dependence on the Wilson coefficients of R_K and R_{K^*} in the bins $[1, 6] \text{ GeV}^2$ and $[1.1, 6] \text{ GeV}^2$, respectively can be expressed as

[11]:

$$R_K = 10^{-2} \left(2.9438 (|C_9|^2 + |C_{10}|^2) - 2\text{Re}(C_9(0.8152 + i0.0892)) + 0.2298 \right), \quad (5.1)$$

$$R_{K^*}^{low} = 10^{-2} \left(3.586 (|C_9|^2 + |C_{10}|^2) - 2\text{Re}(C_9(2.021 + i0.188)) - 2\text{Re}(C_9(5.255 + i0.239)) + 31.658 \right). \quad (5.2)$$

It is clear that a decrease in $R_{K^{(*)}}$ compared to the SM prediction can be achieved only

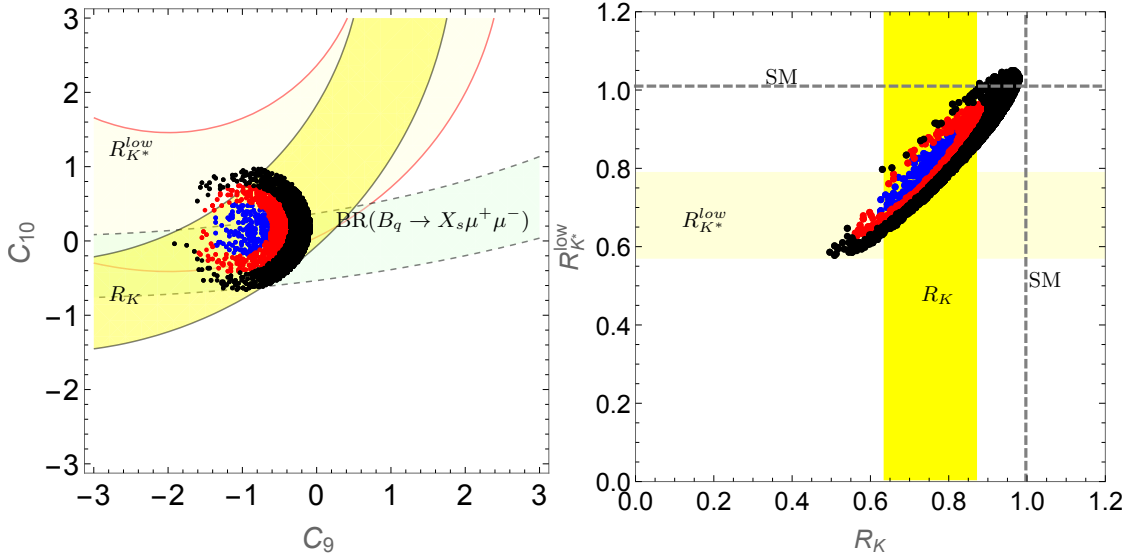


Figure 8. Right: Correlations between R_K and $R_{K^*}^{low}$ in type-III 2HDM by taking all in the text. Left: projection of all constraints in the (C_9, C_{10}) plane.

for $C_{9,10} = 0$. The NP contributions to the Wilson coefficients have further consequences than simply altering the $R_{K^{(*)}}$ observables, and it is crucial to notice that the sizes of $C_{9,10}$ that are allowed in type-III 2HDM in order to accommodate the $R_{K^{(*)}}$ anomalies are also in the region preferred by $b \rightarrow s$ transitions, for instance, $B_q \rightarrow X_s \mu^+ \mu^-$, $B_q \rightarrow \mu^+ \mu^-$ and $B \rightarrow X_s \gamma$. In Fig.8(left), the projected constraints from R_K and $R_{K^*}^{low}$ and together with $B \rightarrow X_s \mu^+ \mu^-$ are shown within the current experimental limit (1σ). The values of $\chi_{ij}^{u,d}$, $\tan \beta$ and m_{H^\pm} varied as in Fig.3, compatible regions were obtained for large $|\chi_{33}^{u,d}|, |\chi_{22}^\mu| \sim 3$ and positive $\chi_{23}^d \sim 1$. Given that $|C_9| \sim |C_{10}|$ is the most preferred scenario, it becomes obvious that $R_K \sim R_{K^*}^{low}$ as shown in the right plot of Fig.8 with the current experimental limit (1σ), and the SM lines are also shown. Interestingly, accommodating the $R_{K^{(*)}}$ implies that the value of R_{B_s} should deviate from the SM prediction by 10% from the central value. A more precise measurement of $B_s \rightarrow \mu^+ \mu^-$ branching fraction will provide more information on C_{10} and so that $R_{K^{(*)}}$.

6 Summary

The recent years of activity at the LHC have brought to light several anomalies in exclusive semileptonic decays. Even though the latest model independent analyses are pointing to sizable NP contributions to different Wilson coefficients. The possibility of interpreting these results in the current situation of the SM is not possible, so it would be worth studying the possibility beyond the SM such as general 2HDM.

In this work, we have studied these anomalies in the context of type-III 2HDM, unlike 2HDM-II, it would be still possible to have relatively light charged scalar in the range 200-400 GeV. By taking constraints from ΔM_q ($q = s, d$), $B \rightarrow X_s \gamma$, $B_s \rightarrow \mu^+ \mu^-$ and $B_q \rightarrow X_s \mu^+ \mu^-$ we have studied the implications of G2HDM on $R_{K^{(*)}}$ to identify how large deviations from the SM predictions are possible.

To obtain compatible $R_{K^{(*)}}$ measured by LHCb, Belle and BaBar a scenario with a large negative C_9 is found due to the charged-scalar exchanges through the Z- and γ -penguin diagrams and under the assumptions of light charged Higgs, large $\tan \beta$ with moderate Yukawa couplings of the order of $\mathcal{O}(1)$. Moreover, of particular interest is the R_{B_s} ratio whose value has been measured to be smaller than its SM prediction by a factor of 10%. In type-III 2HDM we found that $R_{K^{(*)}}$ are predicted to be similar. Finally, future precise measurement of the $R_{K^{(*)}}$ would be very helpful to provide a more definite answer concerning $b \rightarrow s$ transitions at the LHCb, Belle and BaBar collaborations restricting further or even deciphering the NP models.

Acknowledgments

RB was supported in part by Chinese Academy of Sciences (CAS) President's International Fellowship Initiative (PIFI) program (Grant No. 2017VMB0021). This work is supported also by the Moroccan Ministry of Higher Education and Scientific Research MESRSFC and CNRST: Projet PPR/2015/6. CHC was supported by the Ministry of Science and Technology of Taiwan, under grant MOST-106-2112-M-006-010-MY2 (CHC). J.K. Parry was supported by the CAS PIFI program with Grant No. 2016PM020.

A Loop functions

We collect in this appendix the various functions appearing in the processes computed in the text with two variables obtained from the penguin and box diagrams.

$$f_1(x, y) = \frac{x}{72} \left[\frac{7y^2 - 5yx - 8x^2}{(y-x)^3} + \frac{6yx(3x-2y)}{(y-x)^4} \log\left(\frac{y}{x}\right) \right] \quad (\text{A.1})$$

$$f_2(x, y) = \frac{x}{12} \left[\frac{3y-5x}{(y-x)^2} + \frac{2y(3x-2y)}{(x-y)^3} \log\left(\frac{x}{y}\right) \right] \quad (\text{A.2})$$

$$f_3(x, y) = \frac{x}{108} \left[\frac{38y^2 - 79xy + 47x^2}{(y-x)^3} - \frac{6(4y^3 - 6y^2x + 3x^3)}{(y-x)^4} \log\left(\frac{y}{x}\right) \right] \quad (\text{A.3})$$

$$f_4(x, y) = \frac{x}{108} \left[\frac{-37y^2 + 8xy + 53x^2}{(y-x)^4} + \frac{6(2y^3 + 6y^2x - 9yx^2 - 3x^3)}{(y-x)^5} \log\left(\frac{y}{x}\right) \right] \quad (\text{A.4})$$

$$f_5(x, y) = \frac{x}{8(y-x)} \left[\frac{-1}{(y-1)} + \frac{y(1-y)\log(x)}{(y-x)(x-1)(y-1)} - \frac{y(x+1-2y)\log(y)}{(y-x)(y-1)^2} \right] \quad (\text{A.5})$$

$$f_6(x, y) = \frac{x}{16} \left[\frac{-1}{(y-x)} + \frac{x}{(y-x)^2} \log\left(\frac{y}{x}\right) \right] \quad (\text{A.6})$$

$$f_7(x, y) = \frac{x}{8} \left[\frac{(x+2)\log(x)}{(y-x)(x-1)} - \frac{(y+2)\log(y)}{(y-x)(y-1)} \right] \quad (\text{A.7})$$

$$f_8(x, y) = \frac{x^2}{8} \left[\frac{1}{(y-x)} - \frac{y}{(y-x)^2} \log\left(\frac{y}{x}\right) \right] \quad (\text{A.8})$$

$$f_9(x, y) = \frac{x}{16} \left[\frac{y+x}{(y-x)^2} - \frac{2xy}{(y-x)^3} \log\left(\frac{y}{x}\right) \right] \quad (\text{A.9})$$

$$f_{10}(x, y) = \frac{x}{16} \left[\frac{-1}{(y-x)} + \frac{x}{(y-x)^2} \log\left(\frac{y}{x}\right) \right] \quad (\text{A.10})$$

$$f_{11}(x, y) = \frac{x}{8} \left[\frac{(x-2)\log(x)}{(y-x)(x-1)} - \frac{(y-2)\log(y)}{(y-x)(y-1)} \right] \quad (\text{A.11})$$

$$g_1(x, y) = \frac{x}{16} \left[\frac{x-3y}{(y-x)^2} + \frac{2y^2}{(y-x)^3} \log\left(\frac{y}{x}\right) \right] \quad (\text{A.12})$$

$$g_2(x, y) = \frac{x}{216} \left[\frac{38y^2 + 54y^2x - 79yx - 108yx^2 + 47x^2 + 54x^3}{(y-x)^3} \right] \quad (\text{A.13})$$

$$- \frac{6(4y^3 + 9y^3x - 6y^2x - 18y^2x^2 + 9yx^3 + 3x^3)}{(y-x)^4} \log\left(\frac{y}{x}\right) \quad (\text{A.14})$$

$$g_3(x, y) = \frac{3x}{432} \left[\frac{2y^2 + 36y^2x - 7yx - 72yx^2 + 11x^2 + 36x^3}{(y-x)^3} \right] \quad (\text{A.15})$$

$$- \frac{6x(6y^3 - 12y^2x + 6yx^2 + x^2)}{(y-x)^4} \log\left(\frac{y}{x}\right) \quad (\text{A.16})$$

$$g_4(x, y) = \frac{x}{8(y-x)} \left[\frac{x}{x-1} \log(x) - \frac{y}{y-1} \log(y) \right] \quad (\text{A.17})$$

$$g_5(x, y) = \frac{x}{8(y-x)} \left[1 - \frac{y-x^2}{(x-1)(y-x)} \log(x) - \frac{y(x-1)}{(y-1)(y-x)} \log(y) \right] \quad (\text{A.18})$$

$$g_6(x, y) = \frac{x}{8(y-x)} \log\left(\frac{x}{y}\right) \quad (\text{A.19})$$

References

- [1] G. Aad et al. (ATLAS Collaboration), Phys.Lett. **B716**, 1 (2012), [1207.7214](#).
- [2] S. Chatrchyan et al. (CMS Collaboration), Phys.Lett. **B716**, 30 (2012), [1207.7235](#).
- [3] U. Egede, T. Hurth, J. Matias, M. Ramon, and W. Reece, JHEP **0811**, 032 (2008), [0807.2589](#).
- [4] R. Aaij et al. (LHCb collaboration), Phys.Rev.Lett. **111**, 191801 (2013), [1308.1707](#).
- [5] T. L. Collaboration (LHCb) (2015).
- [6] V. Khachatryan *et al.* [CMS Collaboration], Phys. Lett. B **753** (2016) 424, [\[hep-ph/1507.08126\]](#)
- [7] S. Wehle *et al.* [Belle Collaboration], Phys. Rev. Lett. **118** (2017) no.11, 111801, [\[hep-ph/1612.05014\]](#)
- [8] S. Descotes-Genon, T. Hurth, J. Matias, and J. Virto, JHEP **1305**, 137 (2013), [1303.5794](#).
- [9] S. Descotes-Genon, L. Hofer, J. Matias, and J. Virto, JHEP **1412**, 125 (2014), [1407.8526](#).
- [10] W. Altmannshofer and D. M. Straub, Eur. Phys. J. C **75** (2015) no.8, 382, [\[hep-ph/1411.3161\]](#)
- [11] S. Jger and J. Martin Camalich, Phys. Rev. D **93** (2016) no.1, 014028, [\[hep-ph/1412.3183\]](#)
- [12] R. Aaij et al. (LHCb), JHEP **1307**, 084 (2013), [1305.2168](#).
- [13] R. R. Horgan, Z. Liu, S. Meinel, and M. Wingate, Phys.Rev.Lett. **112**, 212003 (2014), [1310.3887](#).
- [14] R. Horgan, Z. Liu, S. Meinel, and M. Wingate (2015), [1501.00367](#).
- [15] A. Bharucha, D. M. Straub, and R. Zwicky (2015), [1503.05534](#).
- [16] R. Aaij et al. (LHCb collaboration), Phys.Rev.Lett. **113**, 151601 (2014), [1406.6482](#).
- [17] C. Bobeth, G. Hiller, and G. Piranishvili, JHEP **0712**, 040 (2007), [0709.4174](#).
- [18] W. Altmannshofer, C. Niehoff, P. Stangl and D. M. Straub, Eur. Phys. J. C **77** (2017) no.6, 377 doi:10.1140/epjc/s10052-017-4952-0 [arXiv:1703.09189 [hep-ph]].
- [19] W. Altmannshofer and D. M. Straub (2015), [1503.06199](#).
- [20] T. Hurth, F. Mahmoudi and S. Neshatpour, JHEP **1412**, 053 (2014) doi:10.1007/JHEP12(2014)053 [arXiv:1410.4545 [hep-ph]].
- [21] G. Hiller and M. Schmaltz, Phys. Rev. D **90**, 054014 (2014) doi:10.1103/PhysRevD.90.054014 [arXiv:1408.1627 [hep-ph]].
- [22] S. Descotes-Genon, J. Matias, and J. Virto, Phys.Rev. **D88**, 074002 (2013), [1307.5683](#).
- [23] R. Gauld, F. Goertz, and U. Haisch, Phys.Rev. **D89**, 015005 (2014), [1308.1959](#).
- [24] A. J. Buras and J. Girrbach, JHEP **1312**, 009 (2013), [1309.2466](#).
- [25] R. Gauld, F. Goertz, and U. Haisch, JHEP **1401**, 069 (2014), [1310.1082](#).
- [26] A. J. Buras, F. De Fazio, and J. Girrbach, JHEP **1402**, 112 (2014), [1311.6729](#).
- [27] W. Altmannshofer, S. Gori, M. Pospelov, and I. Yavin, Phys.Rev. **D89**, 095033 (2014), [1403.1269](#).

- [28] A. Crivellin, G. D’Ambrosio and J. Heeck, Phys. Rev. Lett. **114**, 151801 (2015) doi:10.1103/PhysRevLett.114.151801 [arXiv:1501.00993 [hep-ph]].
- [29] A. Crivellin, G. D’Ambrosio, and J. Heeck (2015), [1503.03477](#).
- [30] C. Niehoff, P. Stangl, and D. M. Straub (2015), [1503.03865](#).
- [31] D. A. Sierra, F. Staub, and A. Vicente (2015), [1503.06077](#).
- [32] A. Celis, J. Fuentes-Martin, M. Jung, and H. Serodio (2015), [1505.03079](#).
- [33] D. Becirevic, S. Fajfer, and N. Kosnik (2015), [1503.09024](#).
- [34] I. d. M. Varzielas and G. Hiller (2015), [1503.01084](#).
- [35] S. L. Glashow, D. Guadagnoli and K. Lane, Phys. Rev. Lett. **114**, 091801 (2015) doi:10.1103/PhysRevLett.114.091801 [arXiv:1411.0565 [hep-ph]].
- [36] S. M. Boucenna, J. W. F. Valle and A. Vicente, Phys. Lett. B **750**, 367 (2015) doi:10.1016/j.physletb.2015.09.040 [arXiv:1503.07099 [hep-ph]].
- [37] C. Bobeth, T. Ewerth, F. Kruger and J. Urban, Phys. Rev. D **64**, 074014 (2001) doi:10.1103/PhysRevD.64.074014 [hep-ph/0104284].
- [38] M. Jung, X. Q. Li and A. Pich, JHEP **1210** (2012) 063 doi:10.1007/JHEP10(2012)063 [arXiv:1208.1251 [hep-ph]].
- [39] Q. Y. Hu, X. Q. Li and Y. D. Yang, Eur. Phys. J. C **77** (2017) no.3, 190 doi:10.1140/epjc/s10052-017-4748-2 [arXiv:1612.08867 [hep-ph]].
- [40] P. Arnan, D. Beirevi, F. Mescia and O. Sumensari, arXiv:1703.03426 [hep-ph].
- [41] G. C. Branco, P. M. Ferreira, L. Lavoura, M. N. Rebelo, M. Sher and J. P. Silva, Phys. Rept. **516**, 1 (2012) doi:10.1016/j.physrep.2012.02.002 [arXiv:1106.0034 [hep-ph]].
- [42] J. F. Gunion, H. E. Haber, G. L. Kane and S. Dawson, Front. Phys. **80**, 1 (2000).
- [43] T. P. Cheng and M. Sher, Phys. Rev. D **35**, 3484 (1987).
- [44] R. Alonso, B. Grinstein and J. Martin Camalich, Phys. Rev. Lett. **118**, no. 8, 081802 (2017), [[hep-ph/1611.06676](#)]
- [45] C. Patrignani *et al.* (Particle Data Group), Chin. Phys. C **40**, 100001 (2016).
- [46] A. Lenz *et al.*, Phys. Rev. D **83**, 036004 (2011) [[hep-ph/1008.1593](#)]
- [47] B. Colquhoun *et al.* [HPQCD Collaboration], Phys. Rev. D **91**, no. 11, 114509 (2015) [[hep-lat/1503.05762](#)]
- [48] D. Becirevic *et al.*, Nucl. Phys. B **634**, 105 (2002), [[hep-ph/0112303](#)]
- [49] G. Buchalla, A. J. Buras and M. E. Lautenbacher, Rev. Mod. Phys. **68**, 1125 (1996) [[hep-ph/9512380](#)]
- [50] T. Inami and C. S. Lim, Prog. Theor. Phys. **65**, 297 (1981) Erratum: [Prog. Theor. Phys. **65**, 1772 (1981)].
- [51] J. Urban, F. Krauss, U. Jentschura and G. Soff, Nucl. Phys. B **523**, 40 (1998), [[hep-ph/9710245](#)]
- [52] D. Becirevic, V. Gimenez, G. Martinelli, M. Papinutto and J. Reyes, JHEP **0204**, 025 (2002), [[hep-lat/0110091](#)]

- [53] D. Becirevic, V. Gimenez, G. Martinelli, M. Papinutto and J. Reyes, Nucl. Phys. Proc. Suppl. **106**, 385 (2002), [[hep-lat/0110117](#)]
- [54] A. J. Buras, M. Jamin and P. H. Weisz, Nucl. Phys. B **347**, 491 (1990).
- [55] M. Ciuchini, E. Franco, V. Lubicz, G. Martinelli, I. Scimemi and L. Silvestrini, Nucl. Phys. B **523**, 501 (1998), [[hep-ph/9711402](#)]
- [56] A. J. Buras, M. Misiak and J. Urban, Nucl. Phys. B **586**, 397 (2000), [[hep-ph/0005183](#)]
- [57] J. P. Lees *et al.* [BaBar Collaboration], Phys. Rev. Lett. **112**, 211802 (2014) doi:10.1103/PhysRevLett.112.211802 [arXiv:1312.5364 [hep-ex]].
- [58] C. Patrignani *et al.* [Particle Data Group], Chin. Phys. C **40** (2016) no.10, 100001. doi:10.1088/1674-1137/40/10/100001
- [59] Y. Amhis *et al.*, [[hep-ph/1612.07233](#)]
- [60] M. Czakon, P. Fiedler, T. Huber, M. Misiak, T. Schutzmeier and M. Steinhauser, JHEP **1504**, 168 (2015), [[hep-ph/1503.01791](#)]
- [61] M. Misiak *et al.*, Phys. Rev. Lett. **114**, no. 22, 221801 (2015), [[hep-ph/1503.01789](#)]
- [62] F. Borzumati and C. Greub, Phys. Rev. D **58**, 074004 (1998), [[hep-ph/9802391](#)]
- [63] M. Ciuchini, G. Degrossi, P. Gambino and G. F. Giudice, Nucl. Phys. B **527**, 21 (1998), [[hep-ph/9710335](#)]
- [64] F. Borzumati and C. Greub, Phys. Rev. D **59**, 057501 (1999), [[hep-ph/9809438](#)]
- [65] T. Hermann, M. Misiak and M. Steinhauser, JHEP **1211**, 036 (2012), [[hep-ph/1208.2788](#)]
- [66] M. Blanke, A. J. Buras, K. Gemmler and T. Heidsieck, JHEP **1203**, 024 (2012), [[hep-ph/1111.5014](#)]
- [67] M. Misiak and M. Steinhauser, Eur. Phys. J. C **77**, no. 3, 201 (2017), [[hep-ph/1702.04571](#)]
- [68] K. G. Chetyrkin, M. Misiak and M. Munz, Phys. Lett. B **400**, 206 (1997), Erratum: [Phys. Lett. B **425**, 414 (1998)], [[hep-ph/9612313](#)]
- [69] W. Altmannshofer, P. Ball, A. Bharucha, A. J. Buras, D. M. Straub and M. Wick, JHEP **0901**, 019 (2009), [[hep-ph/0811.1214](#)]
- [70] S. Descotes-Genon, D. Ghosh, J. Matias and M. Ramon, JHEP **1106**, 099 (2011), [[hep-ph/1104.3342](#)]
- [71] C. Bobeth, P. Gambino, M. Gorbahn and U. Haisch, JHEP **0404**, 071 (2004), [[hep-ph/0312090](#)]
- [72] R. Fleischer, R. Jaarsma and G. Tetlalmatzi-Xolocotzi, JHEP **1705** (2017) 156 doi:10.1007/JHEP05(2017)156 [arXiv:1703.10160 [hep-ph]]. R. Fleischer, D. G. Espinosa, R. Jaarsma and G. Tetlalmatzi-Xolocotzi, arXiv:1709.04735 [hep-ph].
- [73] X. Q. Li, J. Lu and A. Pich, JHEP **1406** (2014) 022 doi:10.1007/JHEP06(2014)022 [arXiv:1404.5865 [hep-ph]]. X. Q. Li, J. Lu and A. Pich, Nucl. Part. Phys. Proc. **273-275** (2016) 1411 doi:10.1016/j.nuclphysbps.2015.09.228 [arXiv:1410.4775 [hep-ph]].
- [74] T. Huber, E. Lunghi, M. Misiak and D. Wyler, Nucl. Phys. B **740**, 105 (2006), [[hep-ph/0512066](#)]
- [75] C. Bobeth, M. Misiak and J. Urban, Nucl. Phys. B **574**, 291 (2000), [[hep-ph/9910220](#)]
- [76] R. Aaij *et al.* [LHCb Collaboration], JHEP **1308**, 131 (2013), [[hep-ph/1304.6325](#)]

- [77] R. Aaij *et al.* [LHCb Collaboration], JHEP **1602** (2016) 104, [[hep-ph/1512.04442](#)]
- [78] S. Chatrchyan *et al.* [CMS Collaboration], Phys. Lett. B **727** (2013) 77, [[hep-ph/1308.3409](#)]
- [79] T. Aaltonen *et al.* [CDF Collaboration], Phys. Rev. Lett. **108** (2012) 081807, [[hep-ph/1108.0695](#)]
- [80] J.-T. Wei *et al.* [Belle Collaboration], Phys. Rev. Lett. **103** (2009) 171801, [[hep-ph/0904.0770](#)]
- [81] B. Aubert *et al.* [BaBar Collaboration], Phys. Rev. D **73** (2006) 092001, [[hep-ex/0604007](#)]
- [82] S. Descotes-Genon, L. Hofer, J. Matias and J. Virto, JHEP **1606** (2016) 092 [[hep-ph/1510.04239](#)]
- [83] F. Beaujean, C. Bobeth and D. van Dyk, Eur. Phys. J. C **74** (2014) 2897 Erratum: [Eur. Phys. J. C **74** (2014) 3179] doi:10.1140/epjc/s10052-014-2897-0, 10.1140/epjc/s10052-014-3179-6 [arXiv:1310.2478 [hep-ph]].
- [84] R. Fleischer, D. G. Espinosa, R. Jaarsma and G. Tetlalmatzi-Xolocotzi, arXiv:1709.04735 [hep-ph].